Received: 28 October 2020 | Revised: 5 July 2021 | Accepted: 10 July 2021

DOI: 10.1111/pce.14151

ORIGINAL ARTICLE

Plant, Cell & Environment WILEY

Transcriptional regulation of *ZIP* genes is independent of local zinc status in Brachypodium shoots upon zinc deficiency and resupply

Sahand Amini[1] | Borjana Arsova[2] | Sylvie Gobert[3,4] | Monique Carnol[5] | Bernard Bosman[5] | Patrick Motte[1] | Michelle Watt[2] | Marc Hanikenne[1]

[1]InBioS - PhytoSystems, Functional Genomics and Plant Molecular Imaging, University of Liège, Liège, Belgium

[2]Root Dynamics Group, IBG-2 – Plant Sciences, Institut für Bio- und Geowissenschaften (IBG), Forschungszentrum Jülich, Jülich, Germany

[3]Laboratory of Oceanology, MARE Center, FOCUS, University of Liège, Liège, Belgium

[4]Station de Recherches Sous-Marines et Océanographiques (STARESO), Pointe de la Revellata, Calvi, France

[5]InBioS - PhytoSystems, Laboratory of Plant and Microbial Ecology, Department of Biology, Ecology, Evolution, University of Liège, Liège, Belgium

Correspondence
Marc Hanikenne, InBioS - PhytoSystems, Functional Genomics and Plant Molecular Imaging, University of Liège, Liège, Belgium.
Email: marc.hanikenne@uliege.be

Present address
Michelle Watt, School of BioSciences, University of Melbourne, Parkville, VIC 3010, Australia

Funding information
FZJ; F.R.S.-FNRS, Grant/Award Numbers: PDR T0120.18, CDR J.0009.17, MIS F.4511.16

Abstract

The biological processes underlying zinc homeostasis are targets for genetic improvement of crops to counter human malnutrition. Detailed phenotyping, ionomic, RNA-Seq analyses and flux measurements with ^{67}Zn isotope revealed whole-plant molecular events underlying zinc homeostasis upon varying zinc supply and during zinc resupply to starved *Brachypodium distachyon* (Brachypodium) plants. Although both zinc deficiency and excess hindered Brachypodium growth, accumulation of biomass and micronutrients into roots and shoots differed depending on zinc supply. The zinc resupply dynamics involved 1,893 zinc-responsive genes. Multiple zinc-regulated transporter and iron-regulated transporter (IRT)-like protein *(ZIP)* transporter genes and dozens of other genes were rapidly and transiently down-regulated in early stages of zinc resupply, suggesting a transient zinc shock, sensed locally in roots. Notably, genes with identical regulation were observed in shoots without zinc accumulation, pointing to root-to-shoot signals mediating whole-plant responses to zinc resupply. Molecular events uncovered in the grass model Brachypodium are useful for the improvement of staple monocots.

KEYWORDS
Brachypodium, deficiency, dynamics, excess, resupply, signalling, zinc, zinc flux

1 | INTRODUCTION

Plants have developed a sophisticated zinc homeostasis network to ensure appropriate zinc supply to tissues throughout their lifetime in varying environments (Choi & Bird, 2014; Clemens, Palmgren, & Kramer, 2002). Zinc is an essential micronutrient with catalytic, regulatory and structural functions in enzymes and proteins (Broadley, White, Hammond, Zelko, & Lux, 2007; Gupta, Ram, & Kumar, 2016). Zinc availability to plants in soils is limited in large areas worldwide (Alloway, 2008), limiting primary productivity and the nutritional quality of agricultural products. Zinc deficiency in plants leads to multiple defects, including lower activity of zinc-binding enzymes, higher reactive oxygen species (ROS) production due in part to reduced ROS-detoxifying copper/zinc superoxide dismutase activity, iron accumulation, membrane and chlorophyll damage and decrease in photosynthetic performance (Vallee & Falchuk, 1993). These defects macroscopically show during growth and development (Broadley et al., 2007; Sinclair & Krämer, 2012). Zinc toxicity from excess exposure can also occur in plants, mostly in anthropogenically perturbed areas (Jensen & Pedersen, 2006). The main zinc toxicity symptoms include reduced growth and yield, iron deficiency and hence chlorosis, as well as interference with magnesium, phosphorus and manganese

uptake and reduced root growth and root hair abnormality (Broadley et al., 2007; Fukao et al., 2011).

Many molecular actors for root zinc uptake and its transport to different organs and organelles have been identified (Ricachenevsky, Menguer, Sperotto, & Fett, 2015; Sinclair & Krämer, 2012). Among them, the zinc-regulated transporter and iron-regulated transporter (IRT)-like protein (ZIP) gene family includes 15 and 12 members in Arabidopsis (*Arabidopsis thaliana*, At) and rice (*Oryza sativa*, Os), 10 and 7 of which are up-regulated in response to zinc deficiency, respectively (Assunção et al., 2010; Huang et al., 2020; Kavitha, Kuruvilla, & Mathew, 2015; Krämer, Talke, & Hanikenne, 2007; Ramesh, Shin, Eide, & Schachtman, 2003; Ricachenevsky et al., 2015; X. Yang, Huang, Jiang, & Zhang, 2009). Although ZIP transporters are widely studied, their specific physiological roles in plant metal homeostasis are not completely understood. Several ZIPs are hypothesized to be responsible for zinc cellular uptake and influx into the cytosol (Colangelo & Guerinot, 2006). However, data on their metal specificity, subcellular localization and individual function remain very fragmentary (Sinclair & Krämer, 2012; Ricachenevsky et al., 2015).

Among the monocotyledonous ZIP transporters involved in zinc, as well as other metal, homeostasis are: rice OsIRT1 (Lee & An, 2009), OsZIP1 (Ramesh et al., 2003), OsZIP4 (Ishimaru et al., 2005), OsZIP5 (Lee et al., 2010) and OsZIP8 (X. Yang et al., 2009), barley HvZIP7 (Tiong et al., 2014) and maize ZmZIP7 (Li et al., 2016). A number of heavy metal ATPases (HMAs) are generally responsible for zinc efflux into the apoplast. The Arabidopsis AtHMA2 and AtHMA4 have an important role in zinc root-to-shoot transport (Hussain et al., 2004). OsHMA2 is apparently the only pump serving this function in rice (Baxter et al., 2003; R. Takahashi et al., 2012). Metal tolerance protein (MTP), major facilitator superfamily (MFS)/zinc-induced facilitator (ZIF), natural resistance–associated macrophage protein (NRAMP), plant cadmium resistance, ATP-binding cassette (ABC), yellow stripe–like (YSL) and vacuolar iron transport (VIT) are other transporter families, few of whose members are involved in zinc and other metal homeostasis in various dicot and monocot species (Hall & Williams, 2003; Ricachenevsky et al., 2015; Sinclair & Krämer, 2012). Moreover, nicotianamine (NA) is an iron, zinc, copper and manganese chelator involved in intracellular, intercellular and long-distance mobility of these metals in monocots and dicots. NA is synthesized by NA synthase (NAS) and in graminaceous monocot plants (i.e., grasses) exclusively, is the precursor for mugineic acid phytosiderophore (PS) synthesis, which are key for iron acquisition but can also bind zinc (Shojima et al., 1990; M. Takahashi et al., 1999). The contribution of the four *NAS* genes in Arabidopsis was characterized in detail (Klatte et al., 2009), and the rice *OsNAS3* gene was demonstrated to be respectively up-regulated and down-regulated by zinc deficiency and excess (Ishimaru et al., 2008; Suzuki et al., 2008), indicating similar functionality.

Sensing and signalling of the zinc status within the plant and in its environment, as well as its integration into a transcriptional regulation of downstream players of the zinc homeostasis network, are poorly understood in plants. The Arabidopsis AtbZIP19 and AtbZIP23 are the main known regulators of zinc homeostasis in plants. Both belong to the basic leucine zipper domain (bZIP)–containing transcription factor (TF) family and regulate the transcription of *ZIP* and *NAS* genes in response to zinc deficiency in Arabidopsis (Assunção et al., 2010). Close homologs from Barley (HvbZIP56 and HvbZIP62, Nazri, Griffin, Peaston, Alexander-Webber, & Williams, 2017), wheat (TabZIPF1 and *TabZIPF4*, Evens, Buchner, Williams, & Hawkesford, 2017) and rice (OsbZIP48 and OsbZIP50, Lilay et al., 2020) could rescue an Arabidopsis *bzip19bzip23* double mutant under zinc deficiency, suggesting a shared function in zinc homeostasis. The Cys-/His-rich motif of the AtbZIP19 and AtbZIP23 proteins is involved in zinc sensing via direct zinc binding, which inactivates these TFs under cellular zinc sufficiency (Assunção et al., 2013; Lilay et al., 2021; Lilay, Castro, Campilho, & Assunção, 2019). In order to discover proteins involved in zinc sensing and signalling in plants, the proteome dynamics upon zinc resupply in zinc-deficient Arabidopsis plants was recently investigated (Arsova et al., 2019). Profiling transcriptome and miRNAome dynamics upon zinc deficiency and zinc resupply for a few days was also shown to have good potential to reveal novel zinc-responsive genes and miRNAs in rice (Bandyopadhyay, Mehra, Hairat, & Giri, 2017; Zeng, Zhang, Ding, & Zhu, 2019).

A large amount of zinc homeostasis research has been carried out on Arabidopsis and then translated to monocotyledonous crop plants. However, Arabidopsis is not the most suitable model to understand zinc homeostasis in monocots, principally because grasses and dicots (a) possess divergent developmental and eventually anatomical features and (b) employ distinct iron uptake strategies, based on either chelated iron(III) or reduced iron(II) uptake, respectively, resulting in distinct interactions with zinc (Hanikenne, Esteves, Fanara, & Rouached, 2021; Kobayashi & Nishizawa, 2012; Marschner, Römheld, & Kissel, 1986). The latter is indeed very important as evidence indicates the interdependence of zinc and iron homeostasis in Arabidopsis (Arsova et al., 2019; Fukao et al., 2011; Pineau et al., 2012; Scheepers et al., 2020; Shanmugam, Tsednee, & Yeh, 2012) and in grasses (Chaney, 1993; Suzuki et al., 2006; Von Wirén, Marschner, & Romheld, 1996). Rice, alternatively, is often used as a model for grasses, but it possesses the unique feature of combining both iron uptake strategies (Ishimaru et al., 2006). Zinc and iron homeostasis in rice is thus not representative of the bulk of other grasses, although zinc and iron cross-homeostasis was also reported in rice (Ishimaru et al., 2008; Kobayashi & Nishizawa, 2012; Ricachenevsky et al., 2011; Saenchai et al., 2016).

In this study, we asked whether novel information on zinc homeostasis in monocots can be obtained by using the grass model *Brachypodium distachyon* (Brachypodium). Being most closely related to wheat and barley among the staple crops, with more similar phenology and root development and anatomy than rice and maize (Watt, Schneebeli, Dong, & Wilson, 2009), the information obtained has potential for easier transfer to valuable crops. Brachypodium combines many attributes of a good model: small and sequenced genome, short life cycle (3–6 weeks), easily transformable and genetically tractable (Brkljacic et al., 2011; The International Brachypodium Initiative, 2010). Brachypodium was previously proposed as a model for

iron and copper homeostasis studies in grasses (Jung, Gayomba, Yan, & Vatamaniuk, 2014; Yordem et al., 2011).

We examined the response of Brachypodium to zinc excess and deficiency, including detailed growth phenotyping. We present commonalities and divergences in zinc homeostasis and its interactions with other metals, iron in particular, between Brachypodium, Arabidopsis and rice. Additionally, ionome and transcriptome dynamics of Brachypodium upon zinc resupply of zinc-deficient plants shed light on striking aspects of zinc homeostasis in this species: a transient down-regulation followed by upregulation of *ZIP* and 83 additional genes in roots at early time-points (10–30 min) upon zinc resupply, assimilated to a local zinc shock response, and a similar response of *ZIP* and 15 other genes in shoots in the absence of zinc accumulation, an indication of rapid root-to-shoot signalling during zinc resupply.

2 | MATERIALS AND METHODS

2.1 | Plant material, growth conditions and zinc isotopic labelling

Brachypodium distachyon Bd21-3 seeds were used (The International Brachypodium Initiative, 2010). De-husked seeds were surface-sterilized by 70% ethanol for 30 seconds and 50% sodium hypochlorite and 0.1% Triton X-100 for 5 min. After five washings with sterile water, seeds were stratified in sterile water in the dark for 1 week at 4°C. Thereafter, seeds were germinated in the dark at room temperature on wet filter paper for 3 days (Figure S1A). Upon germination, seedlings were transplanted in hydroponic trays and control modified Hoagland medium containing 1 μM zinc ($ZnSO_4$) and 10 μM Fe(III)-HBED (Scheepers et al., 2020) for 1 week (Figure S1B). Then, 10-day-old Brachypodium seedlings were grown in control or treatment conditions in hydroponic media for 3 weeks (Figure S1C). Three static conditions were used: control condition (1.5 μM zinc), deficiency (0 μM zinc) and excess (20 μM zinc). In addition, after 3 weeks of zinc deficiency, zinc-starved plants were resupplied with 1 μM zinc and then harvested 10 min, 30 min, 2 hr or 8 hr post resupply to capture the dynamic response to a change in zinc supply (Figure S1D). Fresh media were replaced each week and last replaced the day before harvest. Harvest took place in a 2 hr window at day end. The growth conditions were 16 hr light per day at 150 μmol m^{-2} s^{-1}, 24°C. In all experiments and conditions, hydroponic trays and solution containers were washed prior use with 6 N hydrochloric acid to eliminate zinc traces. This procedure was applied in three independent experiments, and the replication level of each analysis is detailed in figure legends. In experiment 1, samples were separately collected for (i) root and shoot phenotyping (Figures 1–3 and Figures S2 and S11), (ii) ionome profiling (Figures 4 and 5 and Figures S3 and S4) and (iii) RNA-Sequencing (Figure 6–8 and Figures S5–S8, Table 1, Data S1–S5). Root length measurements were performed using the WinRhizo (Regent Instrument Inc., QC Canada) and PaintRhizo (Nagel et al., 2009) tools. Shoot measurements were performed using a LI-3100C Area Meter (LI-COR, Lincoln, NE). Experiment 2 was performed as experiment 1, with the exception that zinc excess was omitted, for independent confirmation of gene expression profiles (Figure 9). Finally, in experiment 3, static conditions were 0 μM zinc and 1.5 μM zinc as above, and additionally included 1.5 μM of a heavy non-radioactive isotope of zinc (^{67}Zn, Isoflex, San Francisco, CA,

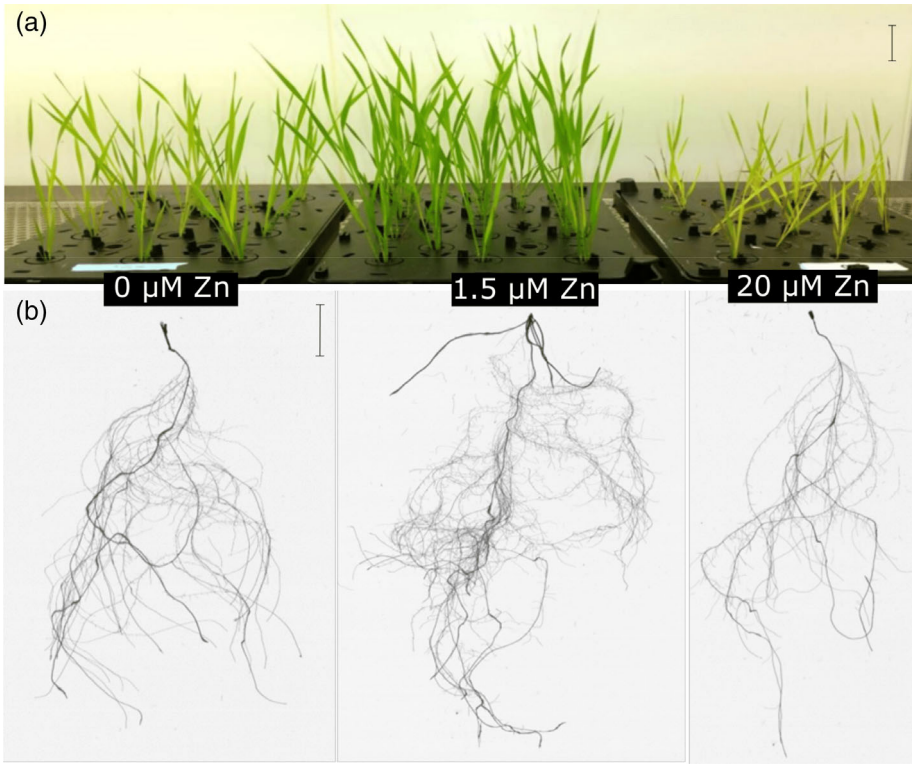

FIGURE 1 Brachypodium plants grown hydroponically in different zinc regimes for 3 weeks. (a) Shoot and (b) representative root images of plants exposed to zinc deficiency (0 μM Zn, left), control (1.5 μM Zn, centre) or excess (20 μM Zn, right) conditions. Pictures are representative of multiple independent experiments. Scale bars are 2 cm [Colour figure can be viewed at wileyonlinelibrary.com]

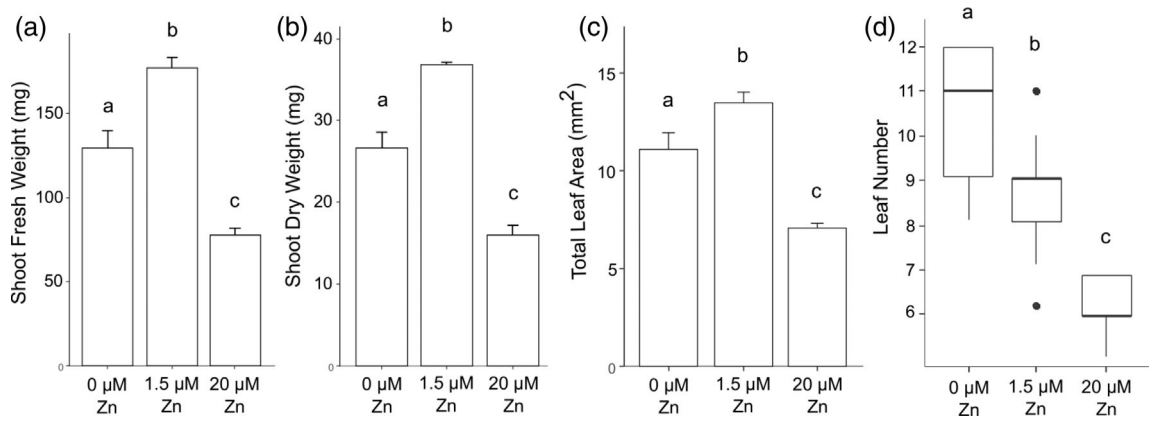

FIGURE 2 Shoot phenotype of Brachypodium plants upon zinc deficiency and excess. Plants grown hydroponically were exposed for 3 weeks to zinc deficiency (0 µM Zn), control (1.5 µM Zn) or excess (20 µM Zn) conditions. (a) Shoot fresh and (b) dry weight. (c) Total leaf area. (a–c) Bars show mean values (+/− standard deviation) of 9–12 individual plants for each treatment. (d) Leaf number per plant. Box and whisker plot showing the median (hardline), interquartile (box), 1.5 interquartile (whiskers) and outliers (dots) of values from 12 individual plants for each treatment. Letters indicate statistical differences (*p*-value <.05) according to Student's *t*-test

catalog Nr. 200,121–01). Zinc-starved plants were resupplied and labelled with 1 µM $^{67}ZnSO_4$ and then harvested at six time-points upon resupply: 10 min, 30 min, 1 hr, 2 hr, 5 hr and 8 hr. The isotope-enriched ^{67}Zn solution (25 mM) was prepared by dissolving metal ingot in diluted H_2SO_4 (Benedicto, Hernández-Apaolaza, Rivas, & Lucena, 2011). In experiment 3, samples were separately collected for (a) isotope concentration analysis and (b) gene expression profiling by quantitative real-time polymerase chain reaction (RT-PCR) (qPCR, Figure 10 and Figures S9 and S10, Data S6).

2.2 | Ionome profiling

Upon harvest, plant root and shoot material were dried at 50°C for 4 days and then digested with nitric acid (Nouet et al., 2015). In experiment 1, ionome profiling was performed by inductively coupled plasma atomic emission spectroscopy (ICP-OES, Vista AX, Varian, Palo Alto, CA; Nouet et al., 2015). In experiment 3, ^{67}Zn, as well as ^{66}Zn, barium and vanadium (as negative controls) concentrations were measured by inductively coupled plasma mass spectrometry using Dynamic Reaction Cell technology (ICP-MS ELAN DRC II, PerkinElmer Inc., Waltham, MA) (Benedicto et al., 2011).

2.3 | Quantitative RT-PCR

Upon harvest, tissues were snap frozen in liquid nitrogen and stored at −80°C. Total RNAs were extracted from root and shoot samples, cDNA preparation and quantitative RT-PCR were conducted as described (Spielmann et al., 2020). Relative transcript level normalization was performed with the $2^{-\Delta\Delta Ct}$ method using *UBC18* (Bradi4g00660) and *EF1α* (Bradi1g06860) reference genes for normalization (Hong, Seo, Yang, Xiang, & Park, 2008). Primer pairs and their efficiency are provided in Table S1.

2.4 | RNA sequencing

Forty-two RNA samples (two tissues: root and shoot, seven conditions: three static and four time-points, each in three biological replicates) from experiment 1 were used for mRNA-Seq library preparation using the TruSeq Stranded mRNA Library Prep Kit (Illumina, San Diego, CA). Libraries were multiplexed and single-end 100 nt RNA-Seq was performed on a Novaseq 6,000 at the GIGA Center (University of Liege, Belgium) yielding on average ~18 million reads per sample. Raw read sequences were archived at NCBI (Bioproject PRJNA669627). The FastQC software v.0.10.1 (http://www.bioinformatics.babraham.ac.uk/projects/fastqc/) was used for assessing read quality. Trimmomatic tool v.0.32 (Bolger, Lohse, & Usadel, 2014) was used for removing sequencing adaptors, polyA and low-quality sequences with the following parameters: remove any reads with base with Q <25 in any sliding window of 10 bases, set crop parameter to 98, leading and trailing to 25 and minimum length to 90 bases. These parameters discarded ~2% of all reads. Using the HISAT2 software v.20.6 (Pertea, Kim, Pertea, Leek, & Salzberg, 2016), reads were mapped on the Brachypodium genome (v.3.2 downloaded from the Phytozome v13 database on 14 February 2020) with max-intronlen 30,000. The average 'overall alignment rate' was 93.87% and 98.51% for root and shoot reads, respectively. Finally, mapped read counts (Data S1) were calculated using HTSEQ-COUNT v.0.6.1p1 (Anders, Pyl, & Huber, 2014).

2.5 | Data analysis

The DESEQ2 package v.1.26.0 in R v.3.6.2 (Love, Huber, & Anders, 2014) was used for normalizing count data, identification of differentially expressed genes (DEG) with a threshold of absolute fold change of +/− 2 and adjusted (Benjamini-Hochberg multiple testing corrected) *p*-value <.05 and for principal component analysis (PCA).

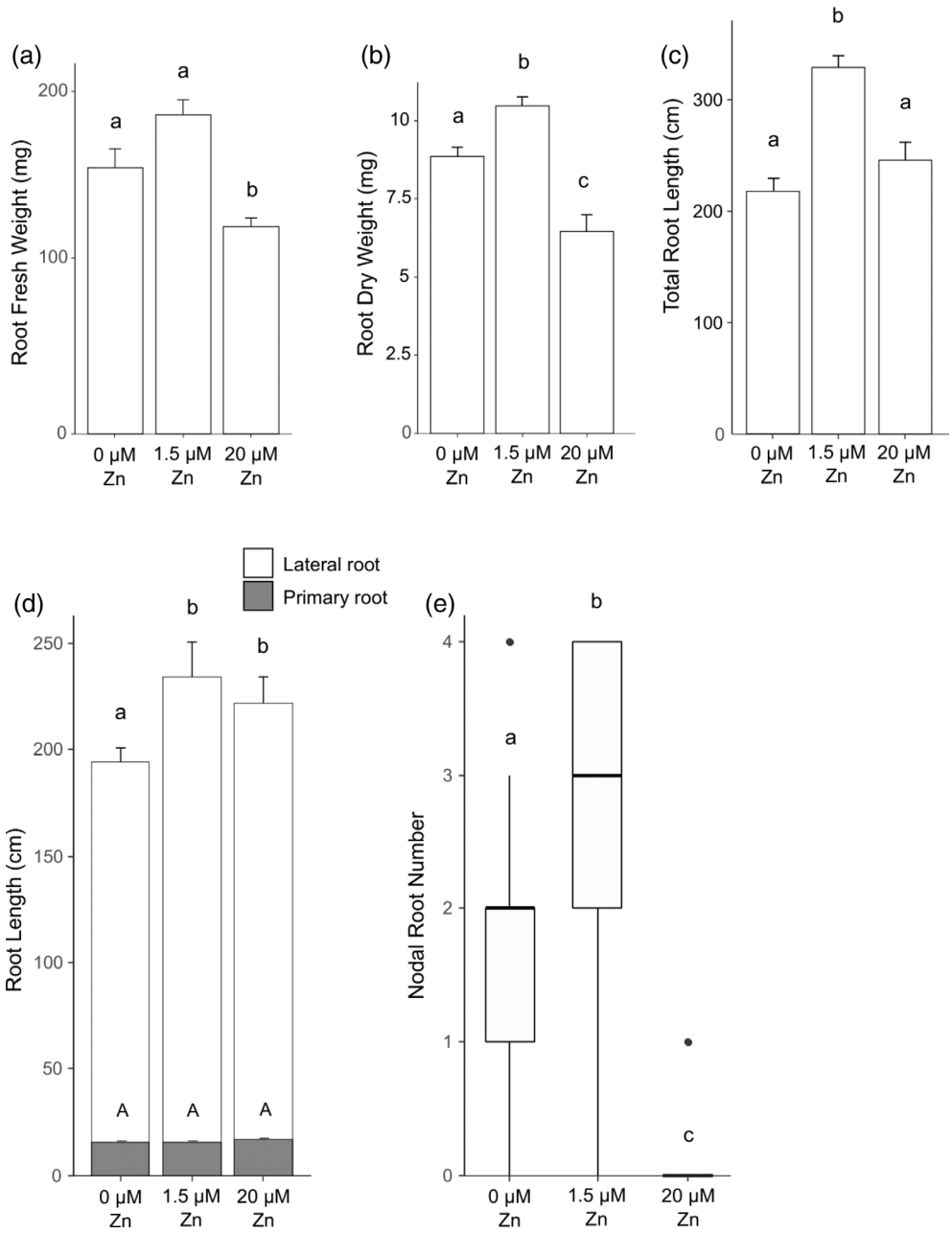

FIGURE 3 Root phenotypic measures of Brachypodium plants under 3 weeks of zinc treatments. Plants grown hydroponically were exposed for 3 weeks to zinc deficiency (0 µM Zn), control (1.5 µM Zn) or excess (20 µM Zn) conditions. (a) Root fresh weight, (b) root dry weight, (c) total root length and (d) primary and lateral root length. (a–d) Bars show mean values (+/− standard deviation) of 9–12 individual plants for each treatment. (e) Nodal root number per plant. Box and whisker plot showing the median (hardline), interquartile (box), 1.5 interquartile (whiskers) and outliers (dots) of values from nine individual plants for each treatment. Letters indicate statistical differences (p-value <.05) according to Student's t-test

Gene Ontology (GO) enrichment analysis was performed using the g:GOSt tool embedded in the g:Profiler web server (Raudvere et al., 2019) with threshold of adjusted p-value <.05 and then visualized with R. For DEG k-means clustering; the multiple experiment viewer (MeV) tool was used (Howe, Sinha, Schlauch, & Quackenbush, 2011). Other statistical tests were conducted using analysis of variance (ANOVA) or Student's t-test (see Figure legends).

2.6 | Gene nomenclature

Among metal-related DEG, only *BdHMA1* and *BdHIPP26* were already annotated in the Phytozome database. *ZIP* genes were previously named by Evens et al. (2017) based on a phylogenetic analysis. For the other genes that were unannotated, we used a best reciprocal hit (BRH) approach with the Phytozome BLAST tool, which allowed identifying their closest homologs in Arabidopsis and/or rice, as well as the gene family to which they belonged.

3 | RESULTS

3.1 | Zinc deficiency and excess hindered Brachypodium shoot growth

Zinc deficiency and excess treatments had negative effects on shoots. Zinc-deficient plants were slightly chlorotic and were shorter than control plants (Figure 1a), with 22.7% and 27.6% reduction of shoot

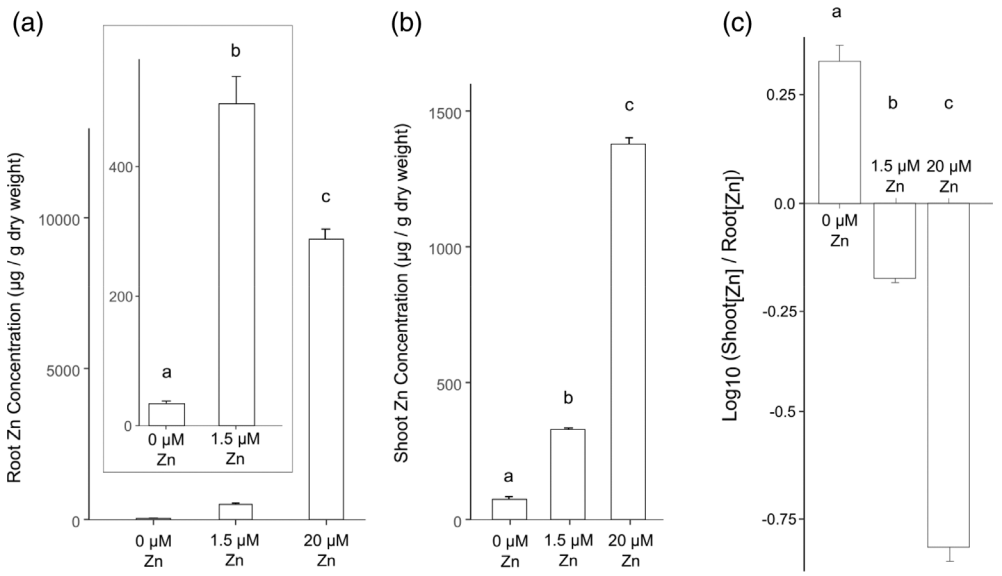

FIGURE 4 Zinc accumulation in roots and shoots of Brachypodium upon zinc deficiency and excess. Plants grown hydroponically were exposed for 3 weeks to zinc deficiency (0 µM Zn), control (1.5 µM Zn) or excess (20 µM Zn) conditions. (a) Root and (b) shoot zinc concentrations. (c) Shoot to root zinc concentration ratio (Log). Bars show mean values (+/− standard deviation) of three biological replicates (three to four plants each). Letters indicate statistical differences (*p*-value <.05) according to Student's *t*-test

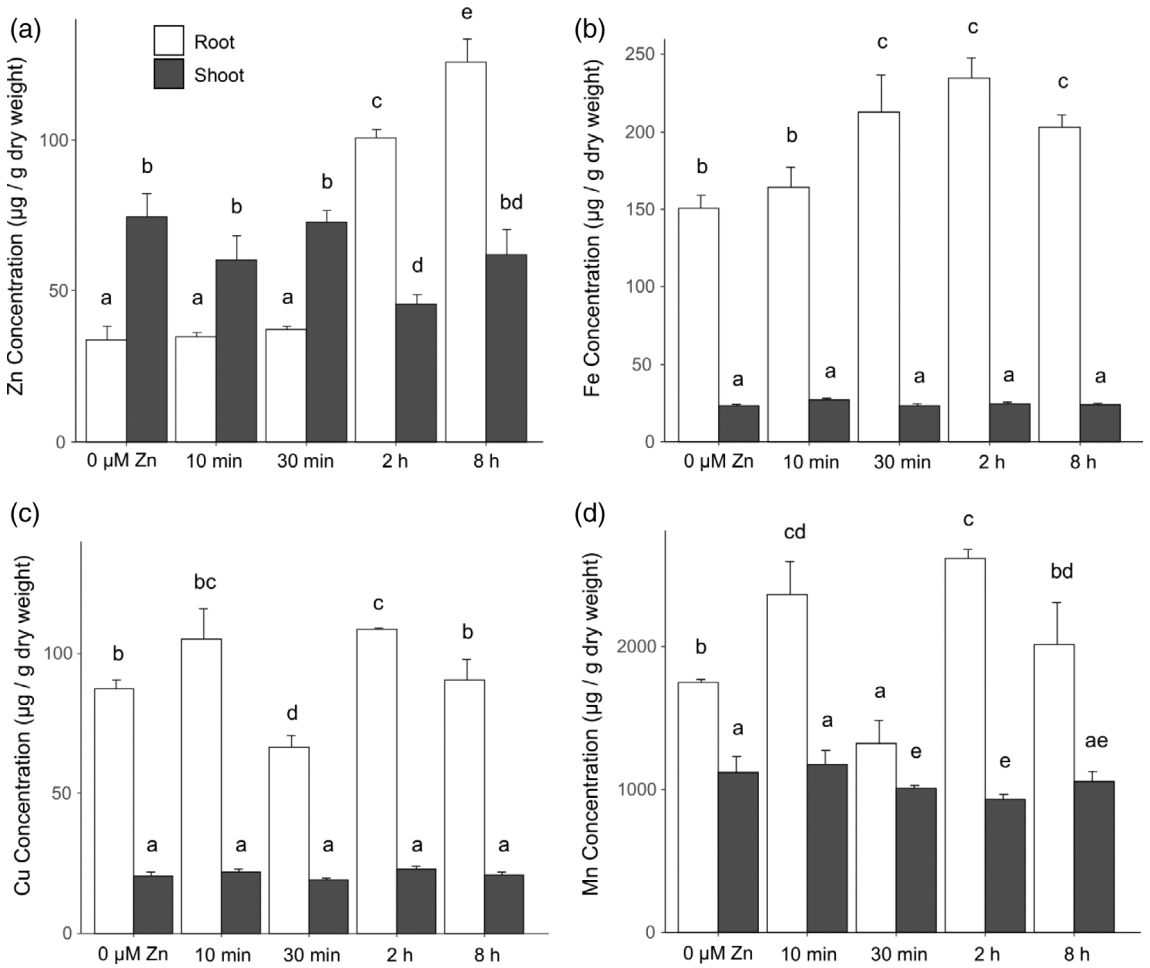

FIGURE 5 Ionome profiling of roots and shoots of Brachypodium upon zinc deficiency and resupply. Plants grown hydroponically under zinc deficiency (0 µM Zn) for 3 weeks were resupplied with 1 µM Zn, and samples were harvested after short time points (10 min to 8 hr). Root and shoot (a) zinc (Zn), (b) iron (Fe), (c) copper (Cu) and (d) manganese (Mn) concentrations. Bars show mean values (+/− standard deviation) of three biological replicates (three to four plants each). Letters indicate statistical differences (*p*-value <.05) according to one-way analysis of variance (ANOVA)

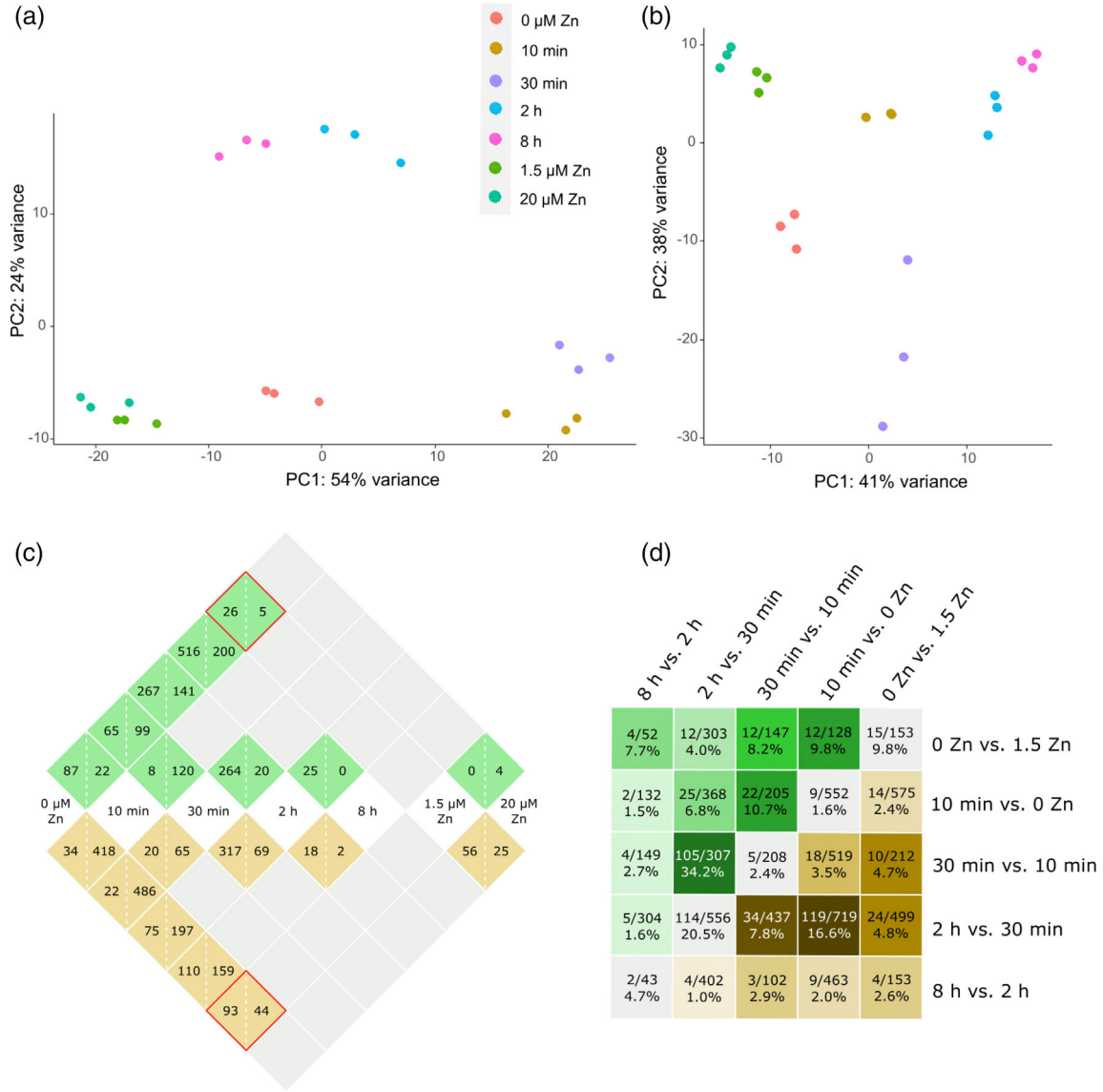

FIGURE 6 RNA sequencing analysis of the steady-state response to zinc deficiency and excess and the dynamic response to zinc deficiency and resupply in Brachypodium. Data are from three biological replicates (three to four plants each) for each treatment. Principal component analysis (PCA) of (a) root and (b) shoot expression data. PCA of root and shoot data together is presented in Figure S5. (c) Number of DEG in nine selected contrasts in roots (brown cells) and in shoots (green cells). Growth conditions are annotated in central white cells and DEG identified in a contrast between two conditions are annotated in the intersecting cell, with numbers of up- (left) and down- (right) regulated genes. For example, in roots, 93 and 44 genes are respectively up- and down-regulated by zinc deficiency (0 µM zinc) compared to the control (1.5 µM zinc) condition (root red square). In shoots, these numbers are respectively 26 and 5 (shoot red square). (d) Ratios of common DEG to the total number of unique DEG for five selected comparisons (deficiency vs. control, and four consecutive comparisons upon zinc resupply) within each tissue are illustrated in green/brown cells. These ratios are also expressed as percentage in each cell. The green upper half of the figure shows shoot data, and the brown lower half shows root data. Colour density illustrates the extent of DEG overlap between two comparisons (a darker colour corresponding to a larger overlap). The grey diagonal cells present ratios of common DEG to the total number of unique DEG in each comparison between root and shoot tissues [Colour figure can be viewed at wileyonlinelibrary.com]

fresh and dry weight (Figure 2a,b), as well as 17.5% smaller total leaf area (Figure 2c). Interestingly, zinc-deficient plants had as median two leaves more than control plants (Figure 2d) but with 26.8% lower dry weight per leaf (Figure S2A).

Similarly, excess zinc impeded shoot growth and caused leaf chlorosis, but with more severe effects than deficiency (Figure 1a). Shoot fresh and dry weight as well as total leaf area were 47.7%–56.2% lower in excess condition compared to control and deficiency, respectively (Figure 2a–c). Plants grown in excess had as median three and five leaves less than control and deficiency plants, respectively (Figure 2d). Finally, dry weight per leaf of zinc excess plants was 34.3% lower than control plants, but the difference with zinc-deficient plants was non-significant (Figure S2A).

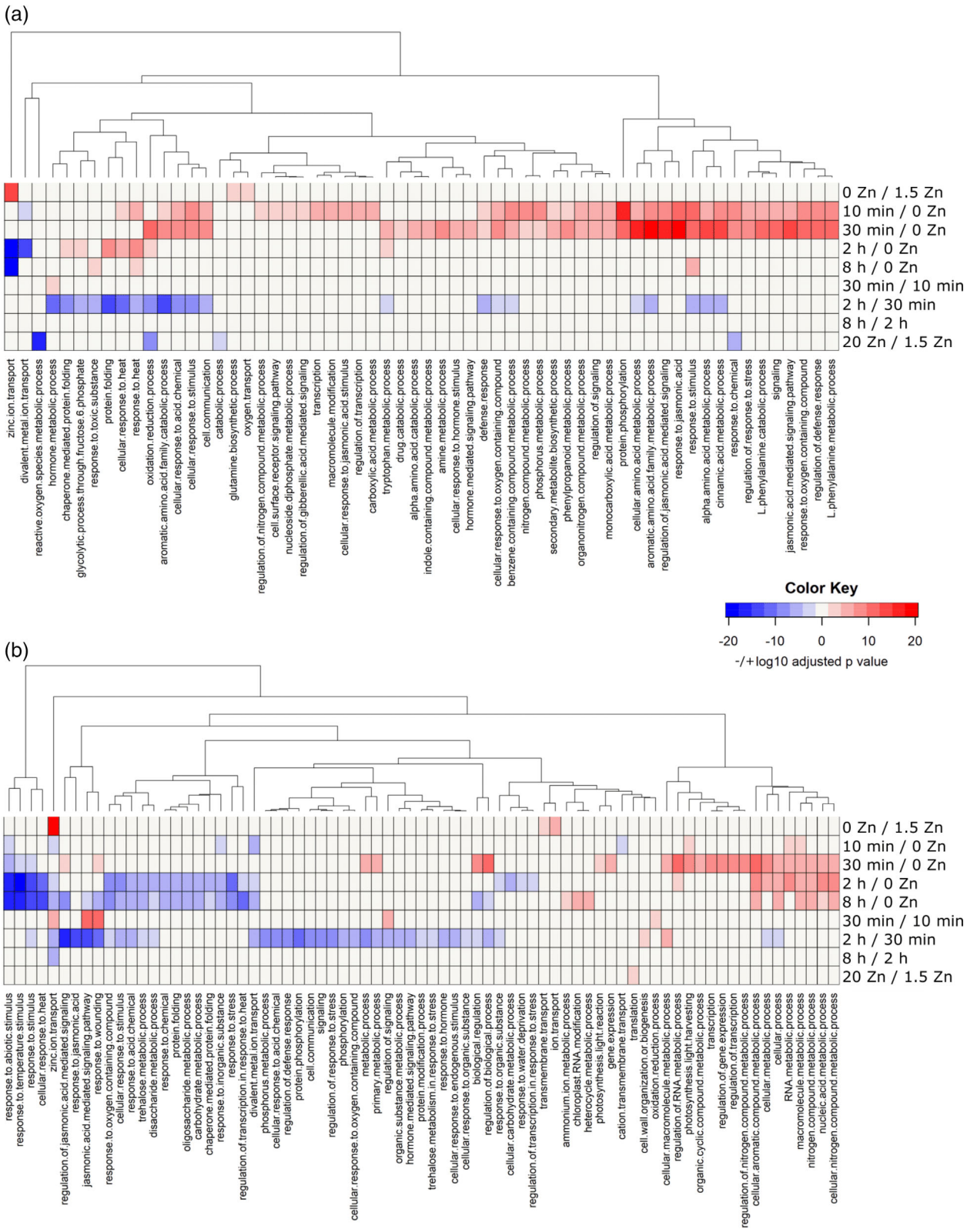

FIGURE 7 Gene Ontology enrichment analysis of the steady-state response to zinc deficiency and excess and the dynamic response to zinc deficiency and resupply in Brachypodium. The heatmaps present statistically enriched (adj. p <.05) Biological processes (BPs) among both up- and down-regulated genes in nine selected contrasts in roots (a) and in shoots (b). Each row shows a contrast. In the heatmap, the colour density indicates the statistical significance of the BP enrichment (−logarithm of adj. p-value), while blue (down) and red (up) colours show the direction of regulation of genes involved in that BP (each BP was specifically only up- or down-regulated with no genes behaving in the opposite direction from that indicated) [Colour figure can be viewed at wileyonlinelibrary.com]

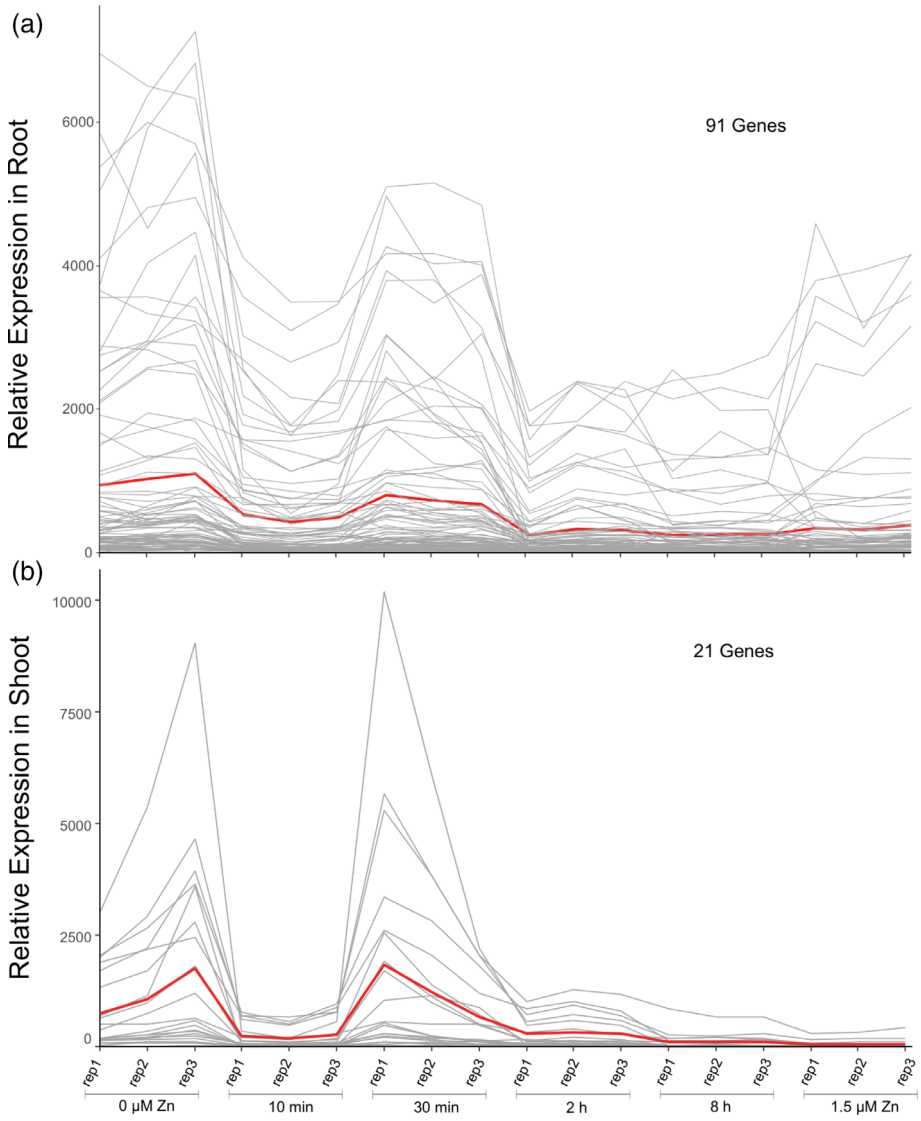

FIGURE 8 Clustering of gene expression upon zinc deficiency and resupply in Brachypodium. Two clusters containing differentially expressed *ZIP* genes in roots (a) and shoots (b) are shown. Pearson correlation was used as distance metric in *k*-means clustering. The number of differentially expressed genes (DEG) included in each cluster is noted in each panel. Full clustering data of root and shoot DEG are shown in Figures S7 and S8, respectively. Lines are there to indicate the expression profile of the genes across the three biological replicates, and they should not be considered as time progression. The red lines show the mean expression of all genes in the cluster [Colour figure can be viewed at wileyonlinelibrary.com]

3.2 | Zinc deficiency and excess altered root phenotypes of Brachypodium plants

The zinc effect on root growth of Brachypodium plants (Figure 1b) differed from shoot responses. Under deficiency, root fresh and dry weight, as well as total root length, were reduced by 15.2%–16.5% (Figure 3a–c). Lateral root length was driving the difference in total root length (Figure 3d), as it was reduced by 17% while primary root lengths were similar under deficiency and control. Zinc-deficient plants had developed one less nodal root (Figure 3e) and lower total nodal root length (Figure S2B) than control plants.

Zinc-excess plants had 22.3%–38% lower fresh and dry root weight than control and zinc-deficient plants (Figure 3a,b), exhibiting stronger responses than the deficiency treatment for these traits. Plants had reduced total root length (Figure 3c) and slightly (but non-significantly) longer primary roots (Figure 3d). Total length of lateral roots of zinc-excess plants was 5.2% lower than control but 14.2% higher than in zinc-deficient plants (Figure 3d). Finally, zinc excess fully inhibited nodal root growth (Figure 3e and Figure S2B).

3.3 | Zinc deficiency and excess impacted the ionome in Brachypodium

Roots and shoots of zinc-deficient plants had 14.7 and 4.4 times lower zinc concentrations than control plants, respectively (Figure 4a, b). Zinc excess caused higher zinc accumulation in roots, with 18.6 times greater concentration than in control plants (Figure 4a). Zinc accumulation in shoots of excess plants was ~4.2 fold higher than in control plants (Figure 4b). Higher zinc supply corresponded to a greater ratio of root to shoot zinc concentration in Brachypodium, indicating different zinc allocation to the tissues under different zinc regimes (Figure 4c).

Zinc deficiency and/or excess also affected iron, manganese, copper, calcium and magnesium concentrations in Brachypodium tissues (Figure S3). Manganese and copper were slightly but significantly less abundant in roots upon deficiency (Figure S3C,E). Root iron and shoot copper concentrations of zinc-deficient plants were 40.7% increased or 25.3% decreased, respectively (Figure S3A,F). Notably, upon zinc excess, manganese and copper root concentrations were 3.4- and

TABLE 1 Nomenclature of metal homeostasis-related genes among differentially expressed genes (DEG) (A) and genes highlighted in the discussion (B)

Brachypodium				Arabidopsis		Rice	
Gene ID	**Description**	**Tissue[a]**	**Cluster #[b]**	**Gene ID**	**Description**	**Gene ID**	**Description**
A. Differentially expressed genes							
Bradi1g53680	ZIP13[c]	Root, shoot	2, 4	AT2G32270	ZIP3	Os07g12890	ZIP8
Bradi2g22520	ZIP5[c]	Root, shoot	2, 4	AT2G32270	ZIP3	Os05g39560	ZIP5
Bradi2g22530	ZIP9[c]	Root, shoot	2, 4	AT2G32270	ZIP3	Os05g39540	ZIP9
Bradi3g17900	ZIP4[c]	Root, shoot	2, 4	AT3G12750	ZIP1	Os08g10630	ZIP4
Bradi2g33110	ZIP7[c]	Root, shoot	2, 4	AT2G30080	ZIP6	Os05g10940	ZIP7
Bradi1g37667	ZIP10[c]	Root, shoot	2, 4	AT1G60960	IRT3	Os06g37010	ZIP10
Bradi1g12860	IRT1[c]	Root	2	AT4G19690	IRT1	Os03g46470	IRT1
Bradi5g21580	ZIP3[c]	Root	2	AT3G12750	ZIP1	Os04g52310	ZIP3
Bradi4g26366	MFS[d]	Root	5	AT5G13740	ZIF1	Os11g04104	MFS antiporter
Bradi4g43620	MFS[d]	Shoot	1	—	—	Os12g03870	MFS antiporter
Bradi5g08250	YSL[d]	Root	1	AT5G41000	YSL4	Os04g32050	YSL6
Bradi5g08260	YSL[d]	Root	1	AT5G41000	YSL4	Os04g32050	YSL6
Bradi1g33347	HMA1[e]	Root	2	AT4G37270	HMA1	Os06g47550	Cd/Zn-transporting ATPase
Bradi1g68950	Zn/Fe transporter[d]	Root	3	AT3G58060	MTP8	Os03g12530	MTP8.1
Bradi4g29720	VIT[d]	Root	2	AT2G01770	VIT1	Os09g23300	Integral membrane protein
Bradi1g17090	NAS[d]	Root	8	AT5G04950	NAS1	Os07g48980	NAS3
Bradi1g53150	Fe/Mn transporter[d]	Root	9	—	—	Os07g15460	NRAMP6
Bradi5g12456	PCR11-related[d]	Root	7	—	—	—	—
Bradi2g43120	ABC transporter[d]	Root	9	AT1G15520	ABCG40/PDR12	Os01g42380	ABCG36/PDR9
Bradi2g31261	ATX2-related[d]	Root	3	—	—	—	—
Bradi5g04560	HIPP26[e]	Shoot	8	AT5G66110	HIPP27	Os04g17100	HIPP42
Bradi3g55480	ATOX1-related[d]	Root	4	—	—	Os02g57350	—
Bradi3g44820	ATOX1-related[d]	Root	5	AT3G56240	Cu chaperone	—	—
Bradi5g12930	ATOX1-related[d]	Root	4	AT4G05030	Copper transport protein family	—	—
Bradi5g25440	ATOX1-related[d]	Root	4	—	—	Os04g57200	Heavy metal transport/ detoxification protein
Bradi3g27550	ATOX1-related[d]	Root	3	AT2G36950	Heavy metal transport/ detoxification superfamily protein	Os10g30450	HIPP35
Bradi5g12960	ATOX1-related[d]	Root	4	—	—	Os04g39350	Heavy metal–associated domain-containing protein
B. Genes highlighted in the discussion							
Bradi1g38150*	FTL[d]	—	—	—	—	Os06g55290	FTL12
Bradi1g18240*	FPFL[d]	—	—	—	—	Os01g25730	FPFL1
Bradi3g48036*	FTL[d]	—	—	—	—	Os04g48840	FTL6
Bradi1g30140*	BdbZIP9[e]	—	—	AT4G35040	bZIP19	—	—
Bradi1g29920*	BdbZIP8[e]	—	—	—	—	—	—

TABLE 1 (Continued)

Brachypodium				Arabidopsis		Rice	
Gene ID	Description	Tissue[a]	Cluster #[b]	Gene ID	Description	Gene ID	Description
Bradi1g34140*	HMA[d]	—	—	AT4G30110/ AT2G19110	HMA2/HMA4	Os06g70070	HMA2
Bradi4g02570*	bZIP[d]	—	—	—	—	—	—

[a]This column indicates the tissue where the genes were differentially expressed upon zinc treatment.
[b]This column indicates the cluster where the differentially expressed genes were found (see Figures S7 and S8).
[c]ZIP genes were named according to the ZIP family phylogenetic analysis of Evens et al. (2017).
[d]Many genes were unannotated in the Phytozome database (https://phytozome.jgi.doe.gov/pz/portal.html). A best reciprocal hit (BRH) approach with the Phytozome BLAST tool was used, which allowed identifying their closest homologues in Arabidopsis and/or rice, as well as the gene family to which they belonged. Each of these genes is identified by its gene ID (Bradixgxxxxx) and a gene family name, as well as with information about its BRH homologs in Arabidopsis and rice – no information available from the BLAST analysis.
[e]*BdHMA1*, *BdHIPP26*, *BdbZIP8* and *BdbZIP9* were already named in the Phytozome.

2.1-fold reduced compared to control, respectively (Figure S3C,E). Finally, calcium and magnesium were 33% and 35.1% higher in shoots of zinc-excess plants, respectively (Figure S3H,J).

3.4 | Rapid ionome dynamics was observed in Brachypodium roots upon zinc deficiency and resupply

During zinc resupply of zinc-deficient roots, we observed gradual accumulation of zinc through time. Zinc increase was modest and non-significant after 10 and 30 min but reached 3.7-fold after 8 hr (Figure 5a). In contrast to the roots, shoot zinc had no consistent increase within the 8 hr of resupply (Figure 5a).

Zinc resupply affected the whole ionome (Figure 5 and Figure S4). The root iron concentration rose gradually until 2 hr parallel to increased zinc level (Figure 5b). Copper and manganese root concentrations displayed different dynamics to zinc and iron with higher levels after 10 min but a severe and transient drop at the 30 min time-point (Figure 5c,d). Changes in the shoot ionome were minor (Figure 5b–d).

3.5 | Transcriptomic responses to steady-state zinc deficiency and excess and to dynamic zinc deficiency and resupply

PCA of the RNA-Seq data indicated that gene expression variance between biological replicates was very low, with the exception of 30 min resupply shoot samples (Figure 6a,b and Figure S5). In roots (Figure 6a), samples clustered according to root zinc concentration (Figures 4 and 5). Control and zinc-excess samples were similar, and zinc-deficiency samples were distinct (Figure 6a). Samples collected after 10 min and 30 min of resupply were similar but distinct from deficiency samples. The 2 hr and 8 hr resupply samples that contained relatively higher zinc concentrations further clustered separately (Figure 6a). The shoot PCA component(s) affecting sample clustering are more difficult to interpret (Figure 6b), possibly in relation to the delayed zinc shoot accumulation (Figure 5a) and, therefore, lower impact of zinc concentration as a principal component. However, even in shoot, PCA separation between static and resupply samples was clear along PC1, with static conditions on the x-axis left side, while resupply samples were progressing with time towards the right along the x-axis (Figure 6b).

DEG were identified [adjusted p <.05 and $\log_2$(fold change) >1] in a selection of 9 out of 21 possible contrasts between the seven treatments for roots and shoots. The nine contrasts included comparisons of zinc deficiency and excess to the control (two comparisons), of zinc resupply time-points to deficiency (four comparisons) and between consecutive resupply time-points (three comparisons) (Figure 6c). One thousand two hundred fifteen and 976 unique DEG were identified in roots and shoots, respectively. Two hundred ninety-eight genes were common among roots and shoots, meaning that 1,893 unique DEG appeared in nine contrasts (Data S2). The steady-state responses to zinc deficiency and excess mobilized less DEG than the dynamic response to zinc resupply. There was little overlap in the zinc resupply response between roots and shoots (Figure 6d). The transcriptional response to zinc resupply was rapid and massive in roots, with the up- or downregulation of >450 genes within 10 min (Figure 6c), with only a small overlap (2.4%) with the static deficiency response (Figure 6d). This latter figure was higher for shoots (9.8%), but differential expression between deficiency and 10 min of zinc resupply concerned many genes as well. In roots and shoots, the response to zinc resupply continued to mobilize new genes with time, but slowed down, with a remarkably low number of DEG between the 2 and 8 hr time-points (Figure 6c,d).

3.6 | Unique biological pathways were involved in the dynamic response to Zn resupply compared to steady-state zinc deficiency and excess

DEG, up-regulated and down-regulated, were submitted to GO enrichment analyses. Overrepresented biological processes (BPs, p-value <.05) were identified in most contrasts (Figure 7, Data S3).

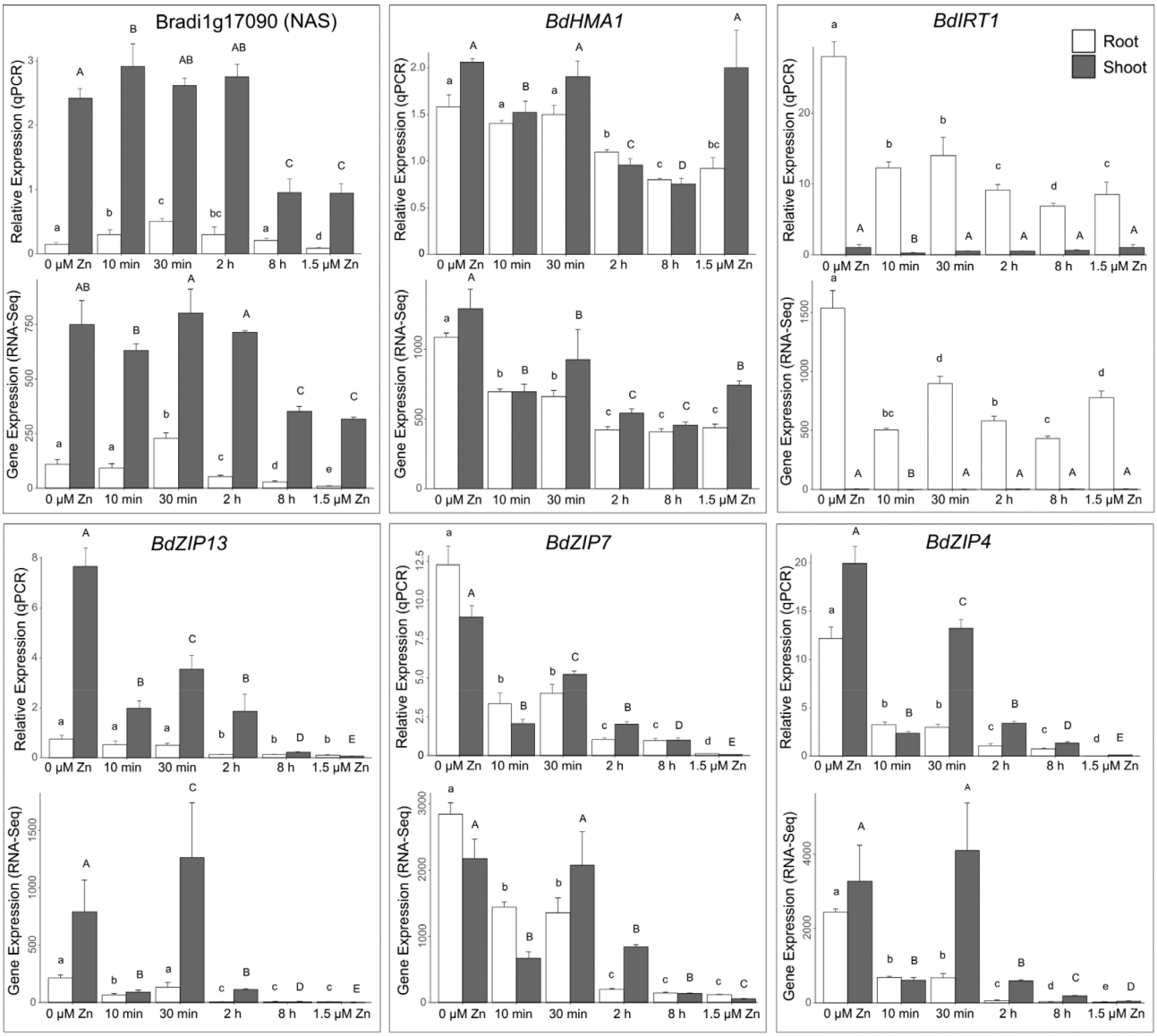

FIGURE 9 Relative expression of metal homeostasis genes upon zinc deficiency and resupply in Brachypodium. RNA sequencing (RNA-Seq, bottom plot) and quantitative real-time polymerase chain reaction (RT-PCR) (qPCR, top plot) transcript levels are compared in roots and shoots for the Bradi1g17090 (NAS family), *BdHMA1*, *BdIRT1*, *BdZIP13*, *BdZIP7* and *BdZIP4* genes. Bars show mean values (+/− standard deviation). qPCR expression levels are relative to *UBC18* and *EF1α* and scaled to average. RNA-Seq and qPCR data are from two fully independent experiments, each consisting of three biological replicates (two to four plants each). Letters indicate statistical differences (p-value <.05) according to one-way analysis of variance (ANOVA)

The 'zinc ion transport' BP was strongly overrepresented among DEG in roots and shoots of deficient plants (0 vs. 1.5 µM zinc), with only up-regulated genes, whereas overrepresentation of catabolism, oxidation–reduction and response to chemical processes were observed in response to excess (20 vs. 1.5 µM zinc) in roots, driven by down-regulated genes only (Figure 7a).

The dynamic response to zinc resupply mobilized many more BPs. In roots, multiple enriched BPs corresponding to up-regulated genes were noticeable (high density red colour, Figure 7a) at the 10 min and/or 30 min time-points compared to deficiency. These BPs were mainly related to signalling, different metabolisms and stress and hormone responses. 'Transcription,' as well as other signalling-related BPs, were enriched only after 10 min resupply. Noticeably, a single enriched BP, 'divalent metal transport,' corresponded to down-regulated genes at 10 min (blue cell at '10 min vs. 0 µM zinc'). This item, as well as 'zinc ion transport,' was also enriched with down-regulated genes (blue cells) after 2 hr of zinc resupply compared to deficiency. As expected, the genes corresponding to the 'zinc ion transport' BP were strongly up-regulated at deficiency but were down-regulated within 2 hr upon resupply. Finally, a single or no BP was enriched in '30 versus 10 min' and '8 versus 2 hr' consecutive time-point comparisons, respectively, whereas a shift in the zinc resupply response was observed between 30 min and 2 ht, with many of the early up-regulated genes being down-

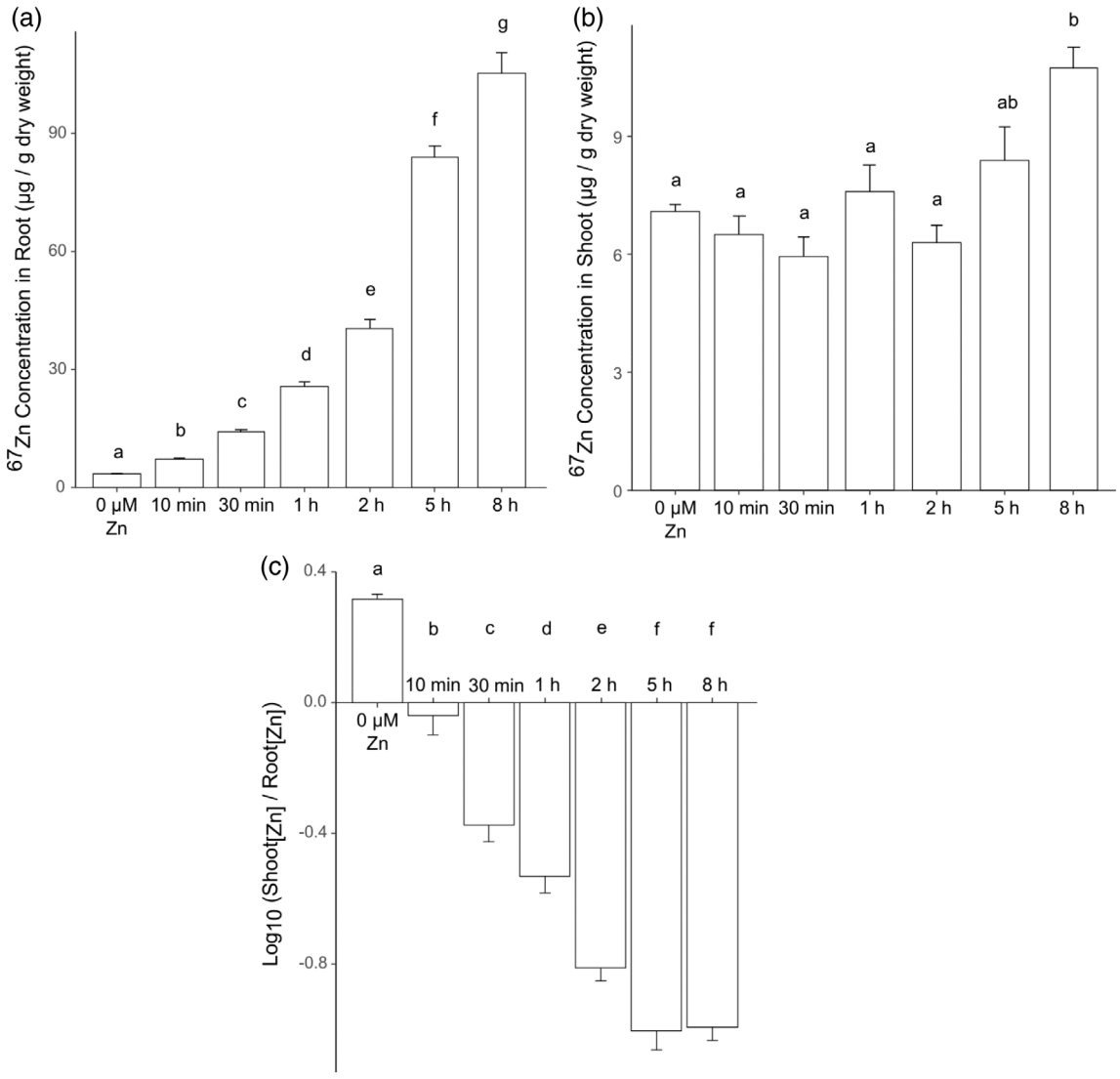

FIGURE 10 ^{67}Zn labelling of Brachypodium plants upon zinc deficiency and resupply. Plants grown hydroponically under zinc deficiency (0 µM Zn) for 3 weeks were resupplied with 1 µM ^{67}Zn, and samples were harvested after short time points (10 min to 8 hr). (a) Root and (b) shoot ^{67}Zn concentrations as determined by inductively coupled plasma mass spectrometry (ICP-MS). (c) Shoot to root ^{67}Zn concentration ratio (Log) throughout the time series upon ^{67}Zn resupply. Bars show mean values (+/− standard deviation) of three biological replicates (four plants each). Letters indicate statistical differences (p-value <.05) according to one-way analysis of variance (ANOVA)

regulated in that interval (see the blue cells in the '2 hr versus 30 min' comparison, Figure 7a).

In shoots (Figure 7b, Data S3), the most striking observation was an enrichment of 'zinc ion transport,' 'divalent metal ion transport' and 'cation transmembrane transport' BPs, corresponding to down-regulated genes within 10 min of resupply, suggesting that a quick transcriptomic regulation of zinc transporter genes preceded zinc re-entry in shoots (Figure 5a). This response was transient as the enriched 'zinc ion transport' BP corresponded to up-regulated genes (30 min) and then down-regulated genes (2 and 8 hr) upon resupply compared to deficiency, respectively. Enriched BPs related to transcription, stress and hormone responses, cellular metabolism and regulation, as well as photosynthesis (Figure 7a, up-regulated BPs, in red), most of which appeared after 10 min resupply in roots, were observed after 30 min in shoots (Figure 7b), that is, with one time-point delay.

3.7 | Genes encoding members of all zinc transporter families were differentially regulated through time and throughout different conditions

Among the 1,893 identified DEG (Figure 6), 27 genes were related to zinc/iron/copper/manganese/cadmium homeostasis/resistance

(Table 1). As Brachypodium is a relatively new model and metal homeostasis studies on this species are scarce, the majority of these annotations was based on sequence or domain similarities with genes/proteins of other species, especially Arabidopsis and rice. Among these 27 genes, 19 genes were differentially expressed in roots only, two in shoots only and six in both tissues (Table 1). The transcriptional regulation of these genes among the nine selected contrasts is provided in Figure S6. The 27 genes belong to families of metal transporters (ZIP [eight genes], MTP [one gene], HMA [one gene], NRAMP [one gene], VIT [one gene], plant cadmium resistance [one gene], ABC transporter [one gene]), metal chelator synthesis (NAS [one gene]) and transport (MFS/ZIF [two genes], YSL [two genes]) or metal chaperones (ATX [one gene]), ATOX1/ heavy-metal-associated isoprenylated plant protein [HIPP] [seven genes]). In general, all known and major zinc transporter families (Ricachenevsky et al., 2015; Sinclair & Krämer, 2012) had thus at least one representative among DEG. However, at least some of the 27 DEG (e.g., Bradi5g08250 and Bradi5g08260 [YSL], Bradi1g53150 [NRAMP]) may be involved not only in zinc, but also in iron, manganese and/or copper homeostasis.

Root and shoot DEG were then clustered according to their expression pattern. Zinc excess was excluded from the analysis as no metal-related genes were regulated in this condition. A total of nine and eight clusters were obtained for roots and shoots, respectively (Figures S7 and S8, Data S4). Metal homeostasis-related genes were distributed in several clusters, with distinct expression patterns, including early or late responses as well as transient regulation, mostly in roots. For instance, root cluster #3 (127 genes) contained three metal homeostasis genes: an MTP (Bradi1g68950) and two copper metallochaperones (Bradi2g31261 and Bradi3g27550) (Data S4). These genes displayed increased gene expression upon zinc resupply, especially at 2 and 8 hr. The six root *ATOX1*-related copper chaperones were distributed in three clusters (#3, #4, #5), which included genes induced with different kinetics during resupply (Figure S7). In contrast, *YSL* family genes clustered together with genes whose expression was intermediate at deficiency and high in control but was transiently repressed during resupply (Cluster #1, Figure S7).

3.8 | Gene clustering showed an unusual temporal regulation of *ZIP* genes upon zinc resupply

Among root clusters (Figure S7), cluster #2 (91 genes) contained all eight differentially expressed *ZIP* genes identified in root samples (Table 1), as well as two other metal-related genes (*BdHMA1* and a VIT family gene, Bradi4g29720) (RootZIP cluster, Data S5). Similarly, among shoot clusters (Figure S8), cluster #4 (21 genes) contained all six *ZIP* genes differentially expressed in shoots (ShootZIP cluster, Data S5). Gene expression patterns in root and shoot ZIP clusters (Figure 8a,b) had a similar shape with two evident peaks of expression at 0 μM zinc and 30 min and a valley at 10 min, resulting in a V-shape consistent with the observation made in the shoot GO enrichment heatmap for the 'zinc ion transport' BP.

3.9 | Shoot *ZIP* transporter genes are down-regulated before measurable amounts of Zn are transported to the shoot

To confirm the V-shape expression pattern of *ZIP* genes (Figure 8), a fully independent experiment with the same design was conducted, except with the exclusion of zinc excess (Experiment 2, Methods). Quantitative RT-PCR was used to profile expression of selected genes: (a) *BdZIP4*, *BdZIP7* and *BdZIP13* present in RootZIP and ShootZIP clusters, (b) *BdIRT1* and *BdHMA1* present in the RootZIP cluster only and (c) the Bradi1g17090 (NAS) gene that was not present in either of these clusters. Complete consistency was observed between RNA sequencing and qPCR data for all six genes in root and shoot tissues in deficiency, resupply and control (Figure 9).

The reproducible V-shape expression pattern of *ZIP* family and 15 other genes in the shoot gene cluster #4 long before zinc influx could be detected in shoots (Figure 5) was puzzling. A possibility was that a tiny amount of zinc was reaching the shoot tissues rapidly, in an amount lower than the ICP-OES detection limit, and was responsible for local transcriptional regulation of these genes. To enable distinction between zinc still present in shoots after 3 weeks of deficiency (~75 ppm, Figure 5a) and resupplied zinc, ^{67}Zn, a non-radioactive zinc isotope, was used for resupply (Experiment 3, Methods). Note that 1- and 5 hr time-points were added to refine the dynamics information. To increase sensitivity and enable detection of zinc isotopes, ^{67}Zn concentration measurements were obtained using ICP-MS.

To ensure that ^{67}Zn has the same physiological effect as naturally abundant zinc, we first analysed zinc-responsive genes by qPCR (Figure S9 compared to Figure 9). The V-shape expression pattern of *BdZIP4*, *BdZIP7* and *BdZIP13* in roots and shoots was again observed. Second, as natural zinc contains a mixture of stable zinc isotopes, with ^{64}Zn being the dominant form and ^{67}Zn representing ~4% (Benedicto et al., 2011), natural zinc supply (1.5 μM) was used as a first negative control (Figure S10A). In line with our expectations, ^{67}Zn concentrations were low when plants were treated with natural zinc and even much lower in deficiency (Figure S10A). Third, ^{66}Zn concentrations in tissues were measured as a second negative control expecting 28% of ^{66}Zn in natural zinc (Benedicto et al., 2011) and 4% ^{66}Zn in ^{67}Zn (based on the provider notice), that is, seven times higher ^{66}Zn in natural zinc than in ^{67}Zn. Accordingly, ^{66}Zn measurements were stable throughout the ^{67}Zn resupply series whereas it was ~7 times higher when plants were treated with natural zinc (Figure S10B), supporting the accuracy of our isotope discrimination by ICP-MS.

Next, ^{67}Zn accumulation in isotope-labelled samples was examined (Figure 10, Data S6). In roots, a gradual and significant increase of ^{67}Zn concentrations was observed with time upon resupply of deficient plants (Figure 10a, Data S6). The gain in sensitivity compared to Experiment 1 was evident: a significant zinc concentration increase was measured from 10 min (Figure 10a), when such a change was only detected after 2 hr in our initial kinetics (Figure 5a). In contrast, ^{67}Zn accumulation in shoots was only detected after 5 hr (Figure 10b). Examining shoot to root ^{67}Zn ratios confirmed that starting from a higher ^{67}Zn shoot accumulation in deficiency, ^{67}Zn resupply mostly

triggered root accumulation up to 5 hr before the ratio stabilized (Figure 10c).

4 | DISCUSSION

In this study, Brachypodium displayed the typical behaviour of a zinc-sensitive, excluder plant (Krämer, 2010). It prioritized shoot zinc accumulation upon deficiency and majorly zinc retention in roots upon excess (Figure 4), in both cases to preserve the photosynthetic function in leaves. This behaviour was very similar to Arabidopsis (Arsova et al., 2019; Talke, Hanikenne, & Krämer, 2006). However, we showed that the molecular pathways used to achieve this are in part different from Arabidopsis, including distinct interactions (iron) and competition (manganese and copper) with other micronutrients, distinct dynamics of zinc transporter genes and distinct local and systemic signalling.

4.1 | Zinc deficiency and excess impact growth and development in Brachypodium

In shoots, increased leaf number was peculiarly associated with reduced total leaf area, total leaf biomass and dry weight per leaf in zinc-deficient plants (Figure 2b–d and Figure S2A). Leaf number is known to be influenced by multiple factors such as flowering time and nutrition (Durand et al., 2012; Hu, Coomer, Loka, Oosterhuis, & Zhou, 2017; MacFarlane & Burchett, 2002). In our RNA-Seq data, three homologs of rice flowering-promoting genes, *OsFTL12* (Bradi1g38150, shoots), *OsFPFL1* (Bradi1g18240, shoots) and *OsFTL6* (Bradi3g48036, roots), were highly up-regulated (7–52 fold) upon zinc deficiency (Data S2). This opens the question of the role of zinc in flowering regulation in Brachypodium. Nutrient deficiency is known to accelerate flowering (Kolář & Seňková, 2008), and flowering is linked with shoot size and leaf number in Arabidopsis, although the effect is variable among early and late flowering ecotypes (X. Chen & Ludewig, 2018). In Brachypodium, clear repression of vegetative growth was associated with increased leaf number. We hypothesize that in order to optimize nutrient-use efficiency in shoot and maintain photosynthesis, plants have adjusted leaf area partitioning (Smith, Sperry, & Adler, 2017).

Root types were affected differentially depending on zinc supply. Deficiency and excess treatments increased lateral root number and length relative to the primary root. Nodal roots, post-embryonic shoot-born roots emerging from consecutive shoot nodes and a unique feature of monocots, were strongly affected. Their initiation was fully inhibited upon zinc excess (Figure 3e). Nodal roots of wheat (Tennant, 1976) are strongly suppressed by low nutrients. In Brachypodium, deprivation of nitrogen, phosphorus (Poiré et al., 2014) and water (Chochois, Voge, Rebetzke, & Watt, 2015) similarly results in a significantly lower number of nodal roots. A positive correlation between nodal root numbers and nutrient uptake, including nitrogen, phosphorus, iron and zinc, is observed in rice (Subedi et al., 2019). Due to a higher diameter of metaxylem to seminal roots and consequent impact on nutrient uptake capacity, nodal roots play a role in nitrate supply to the plant (Liu et al., 2020; Steffens & Rasmussen, 2016). If this is true for zinc too, the observed absence of nodal roots during zinc toxicity can be interpreted as a protective mechanism that minimizes zinc uptake into the plant. However, the decreased number of nodal roots during deficiency does not fully fit into this narrative, unless the development of nodal roots itself has specific zinc requirements. Furthermore, nodal roots provide mechanical stability to the plant (e.g., from winds, Liu et al., 2020), the decreased number or absence of nodal roots in soils with unfavourable zinc conditions may prove to be disadvantageous to logging in various crops and thus further increase yield loss (in addition to the physiological zinc effects). It would therefore be interesting to look for variation in nodal root allocation in response to zinc among Brachypodium accessions, as was found for water supply (Chochois et al., 2015).

4.2 | Interaction of zinc and other metal homeostasis

Zinc excess had no impact on iron root and shoot levels in Brachypodium (Figure S3A), and no enrichment for iron homeostasis genes was observed in the transcriptomic response to zinc excess (Figure 7, Data S2). This contrasts with results from Arabidopsis where zinc excess triggers a secondary iron deficiency with a strong transcriptional response, and zinc toxicity symptoms can be alleviated by higher iron supply (Fukao et al., 2011; Hanikenne et al., 2021; Lešková, Giehl, Hartmann, Fargašová, & von Wirén, 2017; Shanmugam et al., 2012; Zargar et al., 2015). The iron accumulation dynamics in Brachypodium roots was also in contrast to Arabidopsis with a transient increase upon zinc resupply (Figure 5b). Zinc deficiency and resupply instead induces a transient decrease in iron concentration in roots of Arabidopsis (Arsova et al., 2019).

Differences to Arabidopsis studies may be because dicot plants and grasses use distinct iron uptake systems (Kobayashi & Nishizawa, 2012; Hanikenne et al., 2021). In dicot plants such as Arabidopsis, iron uptake is based on a reduction strategy where iron(II) is taken up by IRT1, whereas in grasses, it is based on iron(III) chelation by PS in the rhizosphere prior to PS-iron(III) uptake by roots (Hanikenne et al., 2021; Kobayashi & Nishizawa, 2012). The chelation strategy provides higher uptake specificity and possibly enables less interference by divalent cations such as zinc, although PS were shown to bind zinc in the rhizosphere (Suzuki et al., 2006). None of the genes involved in the chelation strategy in grasses was among zinc-regulated genes in Brachypodium (Data S2). IRT1 homologues are also found in grasses (Evens et al., 2017) and were shown to transport zinc and iron (Ishimaru et al., 2006; Lee & An, 2009; Li et al., 2015). In this study, and in contrast to *OsIRT1* (Ishimaru et al., 2008), *BdIRT1* was regulated by zinc availability (Figure S7). With other ZIPs sharing a similar expression pattern, *BdIRT1* may be

involved in iron and zinc transport and be responsible for higher accumulation of iron upon zinc deficiency (Figure S3A), as well as for the parallel increase of zinc and iron uptake at early time-points upon zinc resupply (Figure 5a,b).

Competition in root uptake between zinc and manganese/copper was possibly regulated by ZIP transporters (Figure S3C,E); however it is still unclear which ZIPs are responsible. In rice and wheat, similar competition with zinc was reported for manganese (Evens et al., 2017; Ishimaru et al., 2008). ZIP, as well as MTP, proteins can indeed potentially transport zinc and manganese (Milner, Seamon, Craft, & Kochian, 2013; Montanini, Blaudez, Jeandroz, Sanders, & Chalot, 2007; Vatansever, Filiz, & Eroglu, 2017). *AtMTP8* and *OsMTP8.1*, although responding to zinc deficiency, are manganese transporters (Z. Chen et al., 2013; Chu et al., 2017). *BdHMA1*, homologue of *AtHMA1* (Kim et al., 2009; Seigneurin-Berny et al., 2006), a RootZIP cluster gene (Figure 8), may mediate zinc/copper interactions. Moreover, among the metal homeostasis genes regulated by zinc in Brachypodium (Table 1, Figure S6), seven are reported to encode proteins related to the human ATOX1 metallochaperone involved in copper chelation (Walker, Tsivkovskii, & Lutsenko, 2002). Annotated as heavy-metal-associated domain–containing proteins, these proteins are also known as *HIPP* genes in plants (de Abreu-Neto, Turchetto-Zolet, de Oliveira, Bodanese Zanettini, & Margis-Pinheiro, 2013). Arabidopsis and rice HIPP homologues were found to be cadmium-responsive and/or involved in copper transport (Shin, Lo, & Yeh, 2012; Zhang et al., 2018).

4.3 | Transcriptional regulation of the Brachypodium zinc response

The AtbZIP19 and AtbZIP23 TFs from Arabidopsis are the best studied regulation system coordinating the zinc deficiency response in plants (Assunção et al., 2010; Lilay et al., 2021). Homologues with conserved functions were characterized in barley, wheat and rice (Castro et al., 2017; Evens et al., 2017; Lilay et al., 2020; Nazri et al., 2017). The Brachypodium homologue of *AtbZIP19*, Bradi1g30140 [annotated as *BdbZIP9* in Phytozome v.12.1, but as *BdbZIP10* or *BdbZIP11* in Glover-Cutter, Alderman, Dombrowski, & Martin, 2014 or Evens et al., 2017] was previously suggested to be involved in a zinc deficiency-induced oxidative stress response (Glover-Cutter et al., 2014; Martin, Vining, & Dombrowski, 2018). However, here, *BdbZIP9* was barely regulated by zinc supply: it was slightly more expressed in zinc-deficient shoots compared to control plants and displayed a very flattened V-shape dynamics upon zinc resupply (Figure S11A). AtbZIP19 and AtbZIP23 are proposed to be specialized in either roots or shoots, respectively (Arsova et al., 2019; Sinclair et al., 2018). *BdbZIP9* was more expressed in shoots than roots (Figure S11A). Interestingly, another *bZIP* gene, Bradi1g29920 (*BdbZIP8* in Phytozome v.12.1), was majorly expressed in roots (Figure S11B) and, although it was not present among initially identified DEG (1.9-fold downregulation 10 min after resupply, Data S1), it displayed the same V-shape expression pattern as ZIP cluster genes upon zinc resupply, suggesting that BdbZIP8 may be involved in zinc homeostasis in Brachypodium.

Additionally, 113 TFs from various families such as WRKY (25 genes), AP2 (24 genes), MYB (22 genes), bHLH (11 genes) and bZIP (nine genes) were among identified DEG (Data S7). None of them is homologues of known zinc regulatory genes.

4.4 | Zinc translocation to the shoot is a slow process

Zinc translocation to shoots was delayed relative to the rapid zinc re-entry in root tissues upon zinc resupply in Brachypodium, similar to earlier observations in Arabidopsis (Arsova et al., 2019). The Arabidopsis AtHMA2 and AtHMA4 pumps, as well as their rice homolog OsHMA2m were shown to be mostly responsible for root-to-shoot zinc transfer (Hussain et al., 2004; Satoh-Nagasawa et al., 2012). Whereas *AtHMA2* expression is induced by zinc deficiency (Arsova et al., 2019; Sinclair et al., 2018), *AtHMA4* and *OsHMA2* expression is barely regulated by zinc (Talke et al., 2006; Wintz et al., 2003; Yamada, Nagano, Nishina, Hara-Nishimura, & Nishimura, 2013). The Brachypodium homologue of these three genes, Bradi1g34140, was moderately induced by zinc deficiency (1.6 fold) in roots, then transiently down-regulated upon zinc resupply before peaking after 8 hr (Figure S11C). This upregulation may be responsible for zinc re-entry observed in shoots after 5 hr of resupply (Figure 10), based on modelling showing that small variations in *HMA4* expression in Arabidopsis suffice to produce large effects in zinc efflux of symplast and to vasculature (Claus, Bohmann, & Chavarría-Krauser, 2013). The Bradi1g34140 late induction upon zinc resupply may therefore be responsible for delayed zinc accumulation in shoots.

In contrast to zinc, copper and manganese concentrations changed quickly upon zinc resupply. Both metals experienced an increase at 10 min and then a decrease at 30 min, the inverse of the V-shape of ZIP clusters in root and shoot, although it was only significant in root (Figure 5c,d). *OsNRAMP5* is suggested to function in manganese distribution from root into shoot (M. Yang et al., 2014). The zinc-responsive *NRAMP* gene (homologue of *OsNRAMP6*, Bradi1g53150) may serve the same function in Brachypodium. Its severe induction at 10 min time-point and with excess zinc, where manganese concentration is lowered (Figure S11D) can support its role in manganese root-to-shoot translocation. On the other hand, *OsATX1*, homologue of *ATOX1*-related copper chaperone, was reported to have an important role in root-to-shoot copper translocation (Zhang et al., 2018) and to interact with multiple rice HMA pumps, probably to transfer copper to these pumps. There are seven *ATOX1*-related genes in the metal list, some of which were immediately regulated by zinc resupply (cluster #4 in Figure S7, cluster #8 in Figure S8). Rapid induction of the Bradi1g53150 (*NRAMP*) gene and several *ATOX1*-related genes (Figure S6), in contrast to the late induction of *AtHMA4* homologue (Bradi1g34140), might explain the efficient regulation of manganese and copper concentration in shoot, compared to zinc.

4.5 | Zinc shock appears to be the first transcriptomic response upon Zn resupply to deficient roots

Expression patterns of the root ZIP cluster genes (Figures 8 and 9) were in stark contrast to observations made in Arabidopsis. In Brachypodium, genes within this cluster were highly expressed at zinc deficiency, rapidly down-regulated after 10 min resupply, then up again after 30 min, thus displaying a V-shape expression pattern (Figures 8 and 9). This response occurred in roots as zinc concentration was steadily increasing upon resupply (Figures 5a and 10a). In Arabidopsis, we observed an initial upregulation in roots of multiple metal homeostasis genes and proteins, including ZIPs, after 10 min of resupply of zinc-starved plant before a downregulation starting after 30 min (Arsova et al., 2019).

The V-shape expression pattern of the ZIP cluster genes in roots implies that zinc influx into roots of zinc-starved plants is sensed as a zinc stress, similar to a zinc excess. Such a zinc shock response was reported in the yeast *Saccharomyces cerevisiae* (MacDiarmid, Milanick, & Eide, 2003; Simm et al., 2007). In yeast, zinc shock was described as a quick and toxic accumulation of high quantities of zinc in cells (MacDiarmid et al., 2003), and it occurs when zinc-limited cells are resupplied with zinc (Simm et al., 2007). Indeed, zinc-limited cells have a high capacity for zinc uptake, and addition of even modest amounts of zinc results in the accumulation of extremely high concentrations of the metal. This zinc shock response in yeast essentially relies on zinc vacuolar storage (Simm et al., 2007).

The observation in Brachypodium differs from yeast in that the perception of the initial zinc influx results in temporal downregulation of zinc transporters, followed by a second (possibly controlled) zinc uptake stage until the zinc demand is met. This is a different and novel strategy enabling the plants to deal with a sudden zinc influx. In Brachypodium, sensing of initial Zn influx indeed initiates, within 10 min, the downregulation of zinc uptake genes in roots. Thereafter, upon sensing yet below-sufficient zinc levels in root tissues, *ZIP* genes are re-up-regulated at 30 min followed by more classical down-regulation with increasing zinc concentrations in tissues at later time-points. The response to zinc resupply in roots therefore occurs in two phases (Figure 6a,d), an initial and rapid phase (10–30 min) combining zinc shock response as well as zinc reuptake supported by intense signalling (Figure 7a), and a later phase (2–8 hr) which corresponds to a slow return to a sufficient state. Although they display very different dynamics, two phases are also observed in response to zinc resupply in Arabidopsis (Arsova et al., 2019).

4.6 | Early transcriptomic response of zinc transporter genes in shoots mirrors the root pattern and is independent of local zinc concentration

Strikingly, shoot ZIP cluster genes (Figures 8 and 9) displayed a V-shape expression pattern as in roots (Figures 8 and 10) although no change in shoot zinc level can be detected within this time-frame (Figures 5a and 10b). In Arabidopsis, no regulation of ZIPs at transcriptional or translational level was observed in shoots before 8 hr of zinc resupply (Arsova et al., 2019). Thus, the early transcriptomic response of zinc transporter genes in shoots appears to be independent of local zinc concentration and to be coordinated with roots in Brachypodium, and we propose that zinc re-entry in roots initiates a root-to-shoot signalling that instigates a distant transcriptomic response (Figure 11).

Shoot transcriptome response, independent from shoot nutrient concentration, was reported upon nitrogen resupply to nitrogen-starved maize plants (Takei, Takahashi, Sugiyama, Yamaya, & Sakakibara, 2002). In roots, several signalling-related BPs were enriched at 10 min and 30 min time-points (Figure 7a, dense red area, up-regulated genes), while this response was delayed in shoots where metal transport (Figure 7b, in blue, down-regulated genes) was among the few enriched BPs after 10 min (Figure 7b). It is therefore tempting to speculate that the root-to-shoot signalling directly represses expression of metal transporter genes in shoot, rather than activating local signalling pathways in shoot. Supporting this idea is that the 'RNA metabolism' BP was also enriched (Figure 7b, in red, up-regulated genes) 10 min after resupply in shoots. Several TFs were found in this enriched BP and belong to different superfamilies such as B3, AP2, WRKY and bZIP (Bradi4g02570, Data S3). These TFs may potentially regulate *ZIP* genes in Brachypodium shoots upon zinc resupply.

Long-distance signalling mechanisms known in plants include electric or hydraulic signalling, calcium waves propagated by calcium-dependent protein kinases and calmodulin proteins, ROS waves, sugar signalling, hormonal signalling and mobile mRNA (Shabala, White, Djordjevic, Ruan, & Mathesius, 2016). Among the signalling-related DEG and enriched BPs at 10 min in root, multiple genes connected to these processes are present and constitute candidates for producing root-to-shoot signals (Data S5).

Long distance or systemic signalling is known to contribute to metal homeostasis regulation. For instance, *AtMTP2* and *AtHMA2* transcript levels in roots are regulated by shoot zinc concentration (i.e., by a systemic signal) in Arabidopsis, in contrast to *ZIP* genes being controlled by the local zinc status (Sinclair et al., 2018). The iron status of the shoot was also shown to control the iron-deficiency response in roots (Mendoza-Cózatl et al., 2014; Vert, Briat, & Curie, 2003; Wang et al., 2007). However, the nature of those signals remains poorly characterized. Designing experiments to identify the nature of our root-to-shoot signalling upon nutrient resupply is a challenge. Indeed, variations of the established split-root experiments (Schikora & Schmidt, 2001; Vert et al., 2003; Wang et al., 2007) or foliar zinc application (Sinclair et al., 2018) will not be informative in the case of a long-distance signal triggered upon resupply of deficient plants as it will either confound nutrient flux and signal or impair the distinction between local and distant responses. Future work will focus on the characterization of the early-responsive signalling genes in roots and on multi-omics analysis of the Brachypodium xylem sap to discern the molecular nature of the signal.

In summary, our study revealed the complexity of the zinc homeostasis network in Brachypodium by comparing static and

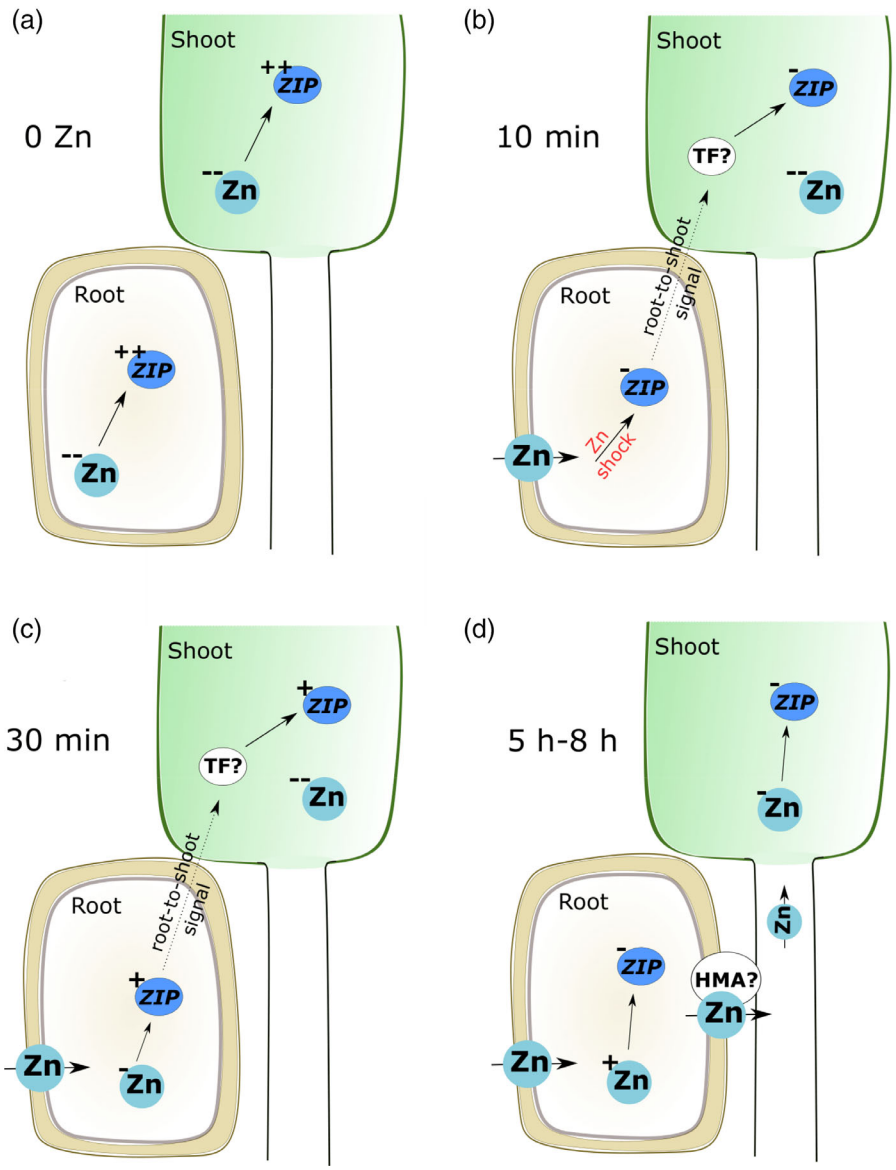

FIGURE 11 Working model of root-to-shoot signalling upon zinc deficiency and resupply in Brachypodium. (a) Zinc deficiency (0 Zn). Depletion of zinc in roots and shoots causes strong upregulation of *ZIP* genes in both tissues. (b) 10 min after zinc resupply (10 min). After a depletion period, zinc resupply is sensed as stress (Zn shock) in roots, which triggers rapid downregulation of *ZIP* gene expression in roots and initiates root-to-shoot signalling. In shoots, *ZIP* genes are also immediately down-regulated although zinc is not transported to shoot yet. (c) 30 min after zinc resupply (30 min). Zinc continues to accumulate in root cells but remains at low concentration. *ZIP* genes are up-regulated again to sustain zinc uptake. This status is signalled to the shoot to induce a similar response. (d) Five to eight hours after zinc resupply (5–8 hr). Zinc concentration keeps increasing which results in the downregulation of *ZIP* genes. At the same time, zinc is translocated to shoot (probably by an HMA homolog, Bradi1g34140) and accumulation of zinc in shoot cells down-regulates *ZIP* genes in shoot as well through local signalling. Double-plus (++) shows very high quantity, plus (+) shows moderate quantity, minus (−) shows low quantity and double-minus (−−) shows very low quantity [Colour figure can be viewed at wileyonlinelibrary.com]

dynamic responses to zinc supply. We identified a short-lived zinc shock response to zinc resupply in roots and hypothetical long-distance zinc signalling that could be important in realistic field resupply conditions. The study also showed that Brachypodium responds phenotypically and genetically to changes in zinc supply and represents a valuable model of staple grass crops to examine zinc homeostasis that contrasts with the widely studied model Arabidopsis. Differences in zinc/iron interactions and in dynamics of transcriptional changes upon zinc resupply reveal the diversity of zinc homeostasis mechanisms among plant species.

ACKNOWLEDGMENTS

Funding was provided by F.R.S.-FNRS grants MIS F.4511.16, CDR J.0009.17 and PDR T0120.18 (Marc Hanikenne). Marie Schloesser, Marie Scheuren, Cédric Delforge, Ana Galinski, Berndt Kastenholz and Tanja Ehrlich are thanked for technical assistance. The GIGA Genomics platform (ULiege) and the Durandal cluster (InBioS-PhytoSystems, ULiege) are thanked for access to sequencing and computational resources, respectively. Sahand Amini is funded by a PhD grant from FZJ. Marc Hanikenne is a Senior Research Associate of F.R.S.-FNRS.

CONFLICT OF INTEREST

The authors declare no conflicts of interest.

AUTHORS' CONTRIBUTIONS

Marc Hanikenne, Sahand Amini and Borjana Arsova designed the research. Sahand Amini performed experiments. Sahand Amini, Marc Hanikenne and Borjana Arsova analysed the data. Sylvie Gobert, Monique Carnol, Bernard Bosman and Patrick Motte contributed to data interpretation. Sahand Amini made the Figures. Sahand Amini, Marc Hanikenne and Borjana Arsova wrote the manuscript with contributions by Michelle Watt. All authors read and approved the manuscript.

DATA AVAILABILITY STATEMENT

The data that support the findings of this study are openly available in the Sequence Read Archive of the NCBI at https://www.ncbi.nlm.nih.gov/sra, with the Bioproject reference number PRJNA669627. The other data are available from the corresponding author upon request.

ORCID

Borjana Arsova https://orcid.org/0000-0002-0566-2009
Marc Hanikenne https://orcid.org/0000-0002-8964-9601

REFERENCES

Alloway, B. J. (2008). Micronutrients and crop production: An introduction. In B. J. Alloway (Ed.), *Micronutrient deficiencies in global crop production* (pp. 1–39). Dordrecht: Springer Netherlands.

Anders, S., Pyl, P. T., & Huber, W. (2014). HTSeq—A python framework to work with high-throughput sequencing data. *Bioinformatics*, *31*(2), 166–169. https://doi.org/10.1093/bioinformatics/btu638

Arsova, B., Amini, S., Scheepers, M., Baiwir, D., Mazzucchelli, G., Carnol, M., … Hanikenne, M. (2019). Resolution of the proteome, transcript and ionome dynamics upon Zn re-supply in Zn-deficient Arabidopsis. *bioRxiv*, 600569. https://doi.org/10.1101/600569

Assunção, A. G., Herrero, E., Lin, Y. F., Huettel, B., Talukdar, S., Smaczniak, C., … Aarts, M. G. M. (2010). *Arabidopsis thaliana* transcription factors bZIP19 and bZIP23 regulate the adaptation to zinc deficiency. *Proceedings of the National Academy of Sciences of the United States of America*, *107*(22), 10296–10301.

Assunção, A. G. L., Persson, D. P., Husted, S., Schjørring, J. K., Alexander, R. D., & Aarts, M. G. M. (2013). Model of how plants sense zinc deficiency. *Metallomics*, *5*(9), 1110–1116. https://doi.org/10.1039/C3MT00070B

Bandyopadhyay, T., Mehra, P., Hairat, S., & Giri, J. (2017). Morpho-physiological and transcriptome profiling reveal novel zinc deficiency-responsive genes in rice. *Functional and Integrative Genomics*, *17*(5), 565–581. https://doi.org/10.1007/s10142-017-0556-x

Baxter, I., Tchieu, J., Sussman, M. R., Boutry, M., Palmgren, M. G., Gribskov, M., … Axelsen, K. B. (2003). Genomic comparison of P-type ATPase ion pumps in Arabidopsis and rice. *Plant Physiology*, *132*(2), 618–628.

Benedicto, A., Hernández-Apaolaza, L., Rivas, I., & Lucena, J. J. (2011). Determination of 67Zn distribution in navy bean (*Phaseolus vulgaris* L.) after foliar application of 67Zn-lignosulfonates using isotope pattern deconvolution. *Journal of Agricultural and Food Chemistry*, *59*(16), 8829–8838. https://doi.org/10.1021/jf2002574

Bolger, A. M., Lohse, M., & Usadel, B. (2014). Trimmomatic: A flexible trimmer for Illumina sequence data. *Bioinformatics*, *30*(15), 2114–2120. https://doi.org/10.1093/bioinformatics/btu170

Brkljacic, J., Grotewold, E., Scholl, R., Mockler, T., Garvin, D. F., Vain, P., … Vogel, J. P. (2011). Brachypodium as a model for the grasses: Today and the future. *Plant Physiology*, *157*(1), 3–13. https://doi.org/10.1104/pp.111.179531

Broadley, M. R., White, P. J., Hammond, J. P., Zelko, I., & Lux, A. (2007). Zinc in plants. *The New Phytologist*, *173*(4), 677–702.

Castro, P. H., Lilay, G. H., Munõz-Mérida, A., Schjoerring, J. K., Azevedo, H., & Assuncaõ, A. G. L. (2017). Phylogenetic analysis of F-bZIP transcription factors indicates conservation of the zinc deficiency response across land plants. *Scientific Reports*, *7*(1), 3806. https://doi.org/10.1038/s41598-017-03903-6

Chaney, R. L. (1993). Zinc Phytotoxicity. In A. D. Robson (Ed.), *Zinc in soils and plants: Proceedings of the international symposium on 'zinc in soils and plants' held at the University of Western Australia, 27–28 September, 1993* (pp. 135–150). Dordrecht: Springer Netherlands.

Chen, X., & Ludewig, U. (2018). Biomass increase under zinc deficiency caused by delay of early flowering in Arabidopsis. *Journal of Experimental Botany*, *69*(5), 1269–1279. https://doi.org/10.1093/jxb/erx478

Chen, Z., Fujii, Y., Yamaji, N., Masuda, S., Takemoto, Y., Kamiya, T., … Ueno, D. (2013). Mn tolerance in rice is mediated by MTP8. 1, a member of the cation diffusion facilitator family. *Journal of Experimental Botany*, *64*, 4375–4387.

Chochois, V., Voge, J. P., Rebetzke, G. J., & Watt, M. (2015). Variation in adult plant phenotypes and partitioning among seed and stem-borne roots across *Brachypodium distachyon* accessions to exploit in breeding cereals for well-watered and drought environments. *Plant Physiology*, *168*(3), 953–967. https://doi.org/10.1104/pp.15.00095

Choi, S., & Bird, A. J. (2014). Zinc'ing sensibly: Controlling zinc homeostasis at the transcriptional level. *Metallomics*, *6*(7), 1198–1215. https://doi.org/10.1039/C4MT00064A

Chu, H.-H., Car, S., Socha, A. L., Hindt, M. N., Punshon, T., & Guerinot, M. L. (2017). The Arabidopsis MTP8 transporter determines the localization of manganese and iron in seeds. *Scientific Reports*, *7*(1), 11024. https://doi.org/10.1038/s41598-017-11250-9

Claus, J., Bohmann, A., & Chavarría-Krauser, A. (2013). Zinc uptake and radial transport in roots of *Arabidopsis thaliana*: A modelling approach to understand accumulation. *Annals of Botany*, *112*, 369–380. https://doi.org/10.1093/aob/mcs263

Clemens, S., Palmgren, M. G., & Kramer, U. (2002). A long way ahead: Understanding and engineering plant metal accumulation. *Trends in Plant Science*, *7*(7), 309–315.

Colangelo, E. P., & Guerinot, M. L. (2006). Put the metal to the petal: Metal uptake and transport throughout plants. *Current Opinion in Plant Biology*, *9*(3), 322–330.

de Abreu-Neto, J. B., Turchetto-Zolet, A. C., de Oliveira, L. F. V., Bodanese Zanettini, M. H., & Margis-Pinheiro, M. (2013). Heavy metal-associated isoprenylated plant protein (HIPP): Characterization of a family of proteins exclusive to plants. *FEBS Journal*, *280*(7), 1604–1616. https://doi.org/10.1111/febs.12159

Durand, E., Bouchet, S., Bertin, P., Ressayre, A., Jamin, P., Charcosset, A., … Tenaillon, M. I. (2012). Flowering time in maize: Linkage and epistasis at a major effect locus. *Genetics*, *190*(4), 1547–1562. https://doi.org/10.1534/genetics.111.136903

Evens, N. P., Buchner, P., Williams, L. E., & Hawkesford, M. J. (2017). The role of ZIP transporters and group F bZIP transcription factors in the Zn-deficiency response of wheat (*Triticum aestivum*). *The Plant Journal*, *92*(2), 291–304. https://doi.org/10.1111/tpj.13655

Fukao, Y., Ferjani, A., Tomioka, R., Nagasaki, N., Kurata, R., Nishimori, Y., … Maeshima, M. (2011). iTRAQ analysis reveals mechanisms of growth defects due to excess zinc in Arabidopsis. *Plant Physiology*, *155*(4), 1893–1907.

Glover-Cutter, K. M., Alderman, S., Dombrowski, J. E., & Martin, R. C. (2014). Enhanced oxidative stress resistance through activation of a zinc deficiency transcription factor in *Brachypodium distachyon*. *Plant Physiology*, *166*(3), 1492–1505. https://doi.org/10.1104/pp.114.240457

Gupta, N., Ram, H., & Kumar, B. (2016). Mechanism of zinc absorption in plants: Uptake, transport, translocation and accumulation. *Reviews in Environmental Science and Bio/Technology*, *15*(1), 89–109. https://doi.org/10.1007/s11157-016-9390-1

Hall, J. L., & Williams, L. E. (2003). Transition metal transporters in plants. *Journal of Experimental Botany*, *54*(393), 2601–2613.

Hanikenne, M., Esteves, S. M., Fanara, S., & Rouached, H. (2021). An iron game: Coordinated homeostasis of essential nutrients. *Journal of Experimental Botany*, *72*(6), 2136–2153. https://doi.org/10.1093/jxb/eraa483

Hong, S. Y., Seo, P. J., Yang, M. S., Xiang, F., & Park, C. M. (2008). Exploring valid reference genes for gene expression studies in *Brachypodium distachyon* by real-time PCR. *BMC Plant Biology*, *8*(1), 1–11. https://doi.org/10.1186/1471-2229-8-112

Howe, E. A., Sinha, R., Schlauch, D., & Quackenbush, J. (2011). RNA-Seq analysis in MeV. *Bioinformatics*, *27*(22), 3209–3210. https://doi.org/10.1093/bioinformatics/btr490

Hu, W., Coomer, T. D., Loka, D. A., Oosterhuis, D. M., & Zhou, Z. (2017). Potassium deficiency affects the carbon-nitrogen balance in cotton leaves. *Plant Physiology and Biochemistry*, *115*, 408–417. https://doi.org/10.1016/j.plaphy.2017.04.005

Huang, S., Sasaki, A., Yamaji, N., Okada, H., Mitani-Ueno, N., & Ma, J. F. (2020). The ZIP transporter family member OsZIP9 contributes to root zinc uptake in rice under zinc-limited conditions. *Plant Physiology*, *183*(3), 1224–1234. https://doi.org/10.1104/pp.20.00125

Hussain, D., Haydon, M. J., Wang, Y., Wong, E., Sherson, S. M., Young, J., … Cobbett, C. S. (2004). P-type ATPase heavy metal transporters with roles in essential zinc homeostasis in Arabidopsis. *Plant Cell*, *16*(5), 1327–1339.

Ishimaru, Y., Suzuki, M., Kobayashi, T., Takahashi, M., Nakanishi, H., Mori, S., & Nishizawa, N. K. (2005). OsZIP4, a novel zinc-regulated zinc transporter in rice. *Journal of Experimental Botany*, *56*(422), 3207–3214.

Ishimaru, Y., Suzuki, M., Ogo, Y., Takahashi, M., Nakanishi, H., Mori, S., & Nishizawa, N. K. (2008). Synthesis of nicotianamine and deoxymugineic acid is regulated by OsIRO2 in Zn excess rice plants. *Soil Science and Plant Nutrition*, *54*(3), 417–423. https://doi.org/10.1111/j.1747-0765.2008.00259.x

Ishimaru, Y., Suzuki, M., Tsukamoto, T., Suzuki, K., Nakazono, M., Kobayashi, T., … Nishizawa, N. K. (2006). Rice plants take up iron as an Fe^{3+}-phytosiderophore and as Fe^{2+}. *The Plant Journal*, *45*(3), 335–346.

Jensen, J., & Pedersen, M. B. (2006). Ecological risk assessment of contaminated soil. *Reviews of Environmental Contamination and Toxicology*, *186*, 73–105. https://doi.org/10.1007/0-387-32883-1_3

Jung, H. I., Gayomba, S. R., Yan, J., & Vatamaniuk, O. K. (2014). *Brachypodium distachyon* as a model system for studies of copper transport in cereal crops. *Frontiers in Plant Science*, *5*, 236. https://doi.org/10.3389/fpls.2014.00236

Kavitha, P. G., Kuruvilla, S., & Mathew, M. K. (2015). Functional characterization of a transition metal ion transporter, OsZIP6 from rice (*Oryza sativa* L.). *Plant Physiology and Biochemistry*, *97*, 165–174. https://doi.org/10.1016/j.plaphy.2015.10.005

Kim, Y. Y., Choi, H., Segami, S., Cho, H. T., Martinoia, E., Maeshima, M., & Lee, Y. (2009). AtHMA1 contributes to the detoxification of excess Zn(II) in Arabidopsis. *The Plant Journal*, *58*, 737–753.

Klatte, M., Schuler, M., Wirtz, M., Fink-Straube, C., Hell, R., & Bauer, P. (2009). The analysis of Arabidopsis nicotianamine synthase mutants reveals functions for nicotianamine in seed iron loading and iron deficiency responses. *Plant Physiology*, *150*(1), 257–271.

Kobayashi, T., & Nishizawa, N. K. (2012). Iron uptake, translocation, and regulation in higher plants. *Annual Review of Plant Biology*, *63*(1), 131–152. https://doi.org/10.1146/annurev-arplant-042811-105522

Kolář, J., & Seňková, J. (2008). Reduction of mineral nutrient availability accelerates flowering of *Arabidopsis thaliana*. *Journal of Plant Physiology*, *165*(15), 1601–1609. https://doi.org/10.1016/j.jplph.2007.11.010

Krämer, U. (2010). Metal hyperaccumulation in plants. *Annual Review of Plant Biology*, *61*, 517–534.

Krämer, U., Talke, I. N., & Hanikenne, M. (2007). Transition metal transport. *FEBS Letters*, *581*, 2263–2272.

Lee, S., & An, G. (2009). Over-expression of OsIRT1 leads to increased iron and zinc accumulations in rice. *Plant, Cell & Environment*, *32*(4), 408–416. https://doi.org/10.1111/j.1365-3040.2009.01935.x

Lee, S., Jeong, H. J., Kim, S. A., Lee, J., Guerinot, M. L., & An, G. (2010). OsZIP5 is a plasma membrane zinc transporter in rice. *Plant Molecular Biology*, *73*(4–5), 507–517.

Lešková, A., Giehl, R. F. H., Hartmann, A., Fargašová, A., & von Wirén, N. (2017). Heavy metals induce iron deficiency responses at different hierarchic and regulatory levels. *Plant Physiology*, *174*(3), 1648–1668. https://doi.org/10.1104/pp.16.01916

Li, S., Zhou, X., Li, H., Liu, Y., Zhu, L., Guo, J., … Chen, R. (2015). Overexpression of ZmIRT1 and ZmZIP3 enhances iron and zinc accumulation in transgenic Arabidopsis. *PLoS One*, *10*(8), e0136647. https://doi.org/10.1371/journal.pone.0136647

Li, S., Zhou, X., Zhao, Y., Li, H., Liu, Y., Zhu, L., … Chen, R. (2016). Constitutive expression of the ZmZIP7 in Arabidopsis alters metal homeostasis and increases Fe and Zn content. *Plant Physiology and Biochemistry*, *106*, 1–10. https://doi.org/10.1016/j.plaphy.2016.04.044

Lilay, G. H., Castro, P. H., Campilho, A., & Assunção, A. G. L. (2019). The Arabidopsis bZIP19 and bZIP23 activity requires zinc deficiency – Insight on regulation from complementation lines. *Frontiers in Plant Science*, *9*, 1955. https://doi.org/10.3389/fpls.2018.01955

Lilay, G. H., Castro, P. H., Guedes, J. G., Almeida, D. M., Campilho, A., Azevedo, H., … Assunção, A. G. L. (2020). Rice F-bZIP transcription factors regulate the zinc deficiency response. *Journal of Experimental Botany*, *71*(12), 3664–3677. https://doi.org/10.1093/jxb/eraa115

Lilay, G. H., Persson, D. P., Castro, P. H., Liao, F., Alexander, R. D., Aarts, M. G., & Assunção, A. G. (2021). Arabidopsis bZIP19 and bZIP23 act as zinc sensors to control plant zinc status. *Nature Plants*, *7*(2), 137–143. https://doi.org/10.1038/s41477-021-00856-7

Liu, Z., Giehl, R. F. H., Hartmann, A., Hajirezaei, M. R., Carpentier, S., & von Wirén, N. (2020). Seminal and nodal roots of barley differ in anatomy, proteome and nitrate uptake capacity. *Plant & Cell Physiology*, *61*(7), 1297–1308. https://doi.org/10.1093/pcp/pcaa059

Love, M. I., Huber, W., & Anders, S. (2014). Moderated estimation of fold change and dispersion for RNA-seq data with DESeq2. *Genome Biology*, *15*(12), 550. https://doi.org/10.1186/s13059-014-0550-8

MacDiarmid, C. W., Milanick, M. A., & Eide, D. J. (2003). Induction of the ZRC1 metal tolerance gene in zinc-limited yeast confers resistance to zinc shock. *The Journal of Biological Chemistry*, *278*(17), 15065–15072.

MacFarlane, G. R., & Burchett, M. D. (2002). Toxicity, growth and accumulation relationships of copper, lead and zinc in the grey mangrove *Avicennia marina* (Forsk.) Vierh. *Marine Environmental Research*, *54*(1), 65–84. https://doi.org/10.1016/S0141-1136(02)00095-8

Marschner, H., Römheld, V., & Kissel, M. (1986). Different strategies in higher plants in mobilization and uptake of iron. *Journal of Plant Nutrition*, *9*(3–7), 695–713. https://doi.org/10.1080/01904168609363475

Martin, R. C., Vining, K., & Dombrowski, J. E. (2018). Genome-wide (ChIP-seq) identification of target genes regulated by BdbZIP10 during paraquat-induced oxidative stress. *BMC Plant Biology*, *18*(1), 58. https://doi.org/10.1186/s12870-018-1275-8

Mendoza-Cózatl, D. G., Xie, Q., Akmakjian, G. Z., Jobe, T. O., Patel, A., Stacey, M. G., … Schroeder, J. I. (2014). OPT3 is a component of the iron-signaling network between leaves and roots and misregulation of OPT3 leads to an over-accumulation of cadmium in seeds. *Molecular Plant*, *7*, 1455–1469. https://doi.org/10.1093/mp/ssu067

Milner, M. J., Seamon, J., Craft, E., & Kochian, L. V. (2013). Transport properties of members of the ZIP family in plants and their role in Zn and Mn homeostasis. *Journal of Experimental Botany*, *64*(1), 369–381. https://doi.org/10.1093/jxb/ers315

Montanini, B., Blaudez, D., Jeandroz, S., Sanders, D., & Chalot, M. (2007). Phylogenetic and functional analysis of the cation diffusion facilitator (CDF) family: Improved signature and prediction of substrate specificity. *BMC Genomics*, *8*(1), 1–16. https://doi.org/10.1186/1471-2164-8-107

Nagel, K. A., Kastenholz, B., Jahnke, S., van Dusschoten, D., Aach, T., Mühlich, M., … Schurr, U. (2009). Temperature responses of roots: Impact on growth, root system architecture and implications for phenotyping. *Functional Plant Biology*, *36*(11), 947–959. https://doi.org/10.1071/FP09184

Nazri, A. Z., Griffin, J. H. C., Peaston, K. A., Alexander-Webber, D. G. A., & Williams, L. E. (2017). F-group bZIPs in barley – A role in Zn deficiency. *Plant, Cell & Environment*, *40*, 2754–2770. https://doi.org/10.1111/pce.13045

Nouet, C., Charlier, J. B., Carnol, M., Bosman, B., Farnir, F., Motte, P., & Hanikenne, M. (2015). Functional analysis of the three *HMA4* copies of the metal hyperaccumulator *Arabidopsis halleri*. *Journal of Experimental Botany*, *66*(19), 5783–5795. https://doi.org/10.1093/jxb/erv280

Pertea, M., Kim, D., Pertea, G. M., Leek, J. T., & Salzberg, S. L. (2016). Transcript-level expression analysis of RNA-seq experiments with HISAT, StringTie and Ballgown. *Nature Protocols*, *11*(9), 1650–1667. https://doi.org/10.1038/nprot.2016.095

Pineau, C., Loubet, S., Lefoulon, C., Chalies, C., Fizames, C., Lacombe, B., … Richard, O. (2012). Natural variation at the *FRD3* MATE transporter locus reveals cross-talk between Fe homeostasis and Zn tolerance in *Arabidopsis thaliana*. *PLoS Genetics*, *8*(12), e1003120. https://doi.org/10.1371/journal.pgen.1003120

Poiré, R., Chochois, V., Sirault, X. R. R., Vogel, J. P., Watt, M., & Furbank, R. T. (2014). Digital imaging approaches for phenotyping whole plant nitrogen and phosphorus response in *Brachypodium distachyon*. *Journal of Integrative Plant Biology*, *56*(8), 781–796. https://doi.org/10.1111/jipb.12198

Ramesh, S. A., Shin, R., Eide, D. J., & Schachtman, D. P. (2003). Differential metal selectivity and gene expression of two zinc transporters from rice. *Plant Physiology*, *133*(1), 126–134. https://doi.org/10.1104/pp.103.026815

Raudvere, U., Kolberg, L., Kuzmin, I., Arak, T., Adler, P., Peterson, H., & Vilo, J. (2019). G:Profiler: A web server for functional enrichment analysis and conversions of gene lists (2019 update). *Nucleic Acids Research*, *47*(W1), W191–W198. https://doi.org/10.1093/nar/gkz369

Ricachenevsky, F. K., Menguer, P. K., Sperotto, R. A., & Fett, J. P. (2015). Got to hide your Zn away: Molecular control of Zn accumulation and biotechnological applications. *Plant Science*, *236*, 1–17. https://doi.org/10.1016/j.plantsci.2015.03.009

Ricachenevsky, F. K., Sperotto, R. A., Menguer, P. K., Sperb, E. R., Lopes, K. L., & Fett, J. P. (2011). ZINC-INDUCED FACILITATOR-LIKE family in plants: Lineage-specific expansion in monocotyledons and conserved genomic and expression features among rice (*Oryza sativa*) paralogs. *BMC Plant Biology*, *11*(1), 20. https://doi.org/10.1186/1471-2229-11-20

Saenchai, C., Bouain, N., Kisko, M., Prom-u-thai, C., Doumas, P., & Rouached, H. (2016). The involvement of OsPHO1;1 in the regulation of iron transport through integration of phosphate and zinc deficiency signalling. *Frontiers in Plant Science*, *7*, 396. https://doi.org/10.3389/fpls.2016.00396

Satoh-Nagasawa, N., Mori, M., Nakazawa, N., Kawamoto, T., Nagato, Y., Sakurai, K., … Akagi, H. (2012). Mutations in Rice (*Oryza sativa*) heavy metal ATPase 2 (OsHMA2) restrict the translocation of zinc and cadmium. *Plant and Cell Physiology*, *53*(1), 213–224. https://doi.org/10.1093/pcp/pcr166

Scheepers, M., Spielmann, J., Boulanger, M., Carnol, M., Bosman, B., De Pauw, E., … Hanikenne, M. (2020). Intertwined metal homeostasis, oxidative and biotic stress responses in the Arabidopsis *frd3* mutant. *The Plant Journal*, *102*, 34–52. https://doi.org/10.1111/tpj.14610

Schikora, A., & Schmidt, W. (2001). Iron stress-induced changes in root epidermal cell fate are regulated independently from physiological responses to low iron availability. *Plant Physiology*, *125*(4), 1679–1687. https://doi.org/10.1104/pp.125.4.1679

Seigneurin-Berny, D., Gravot, A., Auroy, P., Mazard, C., Kraut, A., Finazzi, G., … Rolland, N. (2006). HMA1, a new cu-ATPase of the chloroplast envelope, is essential for growth under adverse light conditions. *The Journal of Biological Chemistry*, *281*(5), 2882–2892.

Shabala, S., White, R. G., Djordjevic, M. A., Ruan, Y.-L., & Mathesius, U. (2016). Root-to-shoot signalling: Integration of diverse molecules, pathways and functions. *Functional Plant Biology*, *43*(2), 87–104. https://doi.org/10.1071/FP15252

Shanmugam, V., Tsednee, M., & Yeh, K.-C. (2012). ZINC TOLERANCE INDUCED BY IRON 1 reveals the importance of glutathione in the cross-homeostasis between zinc and iron in *Arabidopsis thaliana*. *The Plant Journal*, *69*(6), 1006–1017. https://doi.org/10.1111/j.1365-313X.2011.04850.x

Shin, L. J., Lo, J. C., & Yeh, K. C. (2012). Copper chaperone antioxidant Protein1 is essential for copper homeostasis. *Plant Physiology*, *159*(3), 1099–1110. https://doi.org/10.1104/pp.112.195974

Shojima, S., Nishizawa, N. K., Fushiya, S., Nozoe, S., Irifune, T., & Mori, S. (1990). Biosynthesis of phytosiderophores: In vitro biosynthesis of 2′-deoxymugineic acid from L-methionine and nicotianamine. *Plant Physiology*, *93*(4), 1497–1503. https://doi.org/10.1104/pp.93.4.1497

Simm, C., Lahner, B., Salt, D., LeFurgey, A., Ingram, P., Yandell, B., & Eide, D. J. (2007). *Saccharomyces cerevisiae* vacuole in zinc storage and intracellular zinc distribution. *Eukaryotic Cell*, *6*(7), 1166–1177. https://doi.org/10.1128/EC.00077-07

Sinclair, S. A., & Krämer, U. (2012). The zinc homeostasis network of land plants. *Biochimica et Biophysica Acta*, *1823*, 1553–1567. https://doi.org/10.1016/j.bbamcr.2012.05.016

Sinclair, S. A., Senger, T., Talke, I. N., Cobbett, C. S., Haydon, M. J., & Kraemer, U. (2018). Systemic upregulation of MTP2- and HMA2-mediated Zn partitioning to the shoot supplements local Zn deficiency responses of Arabidopsis. *The Plant Cell*, *30*, 2463–2479. https://doi.org/10.1105/tpc.18.00207

Smith, D. D., Sperry, J. S., & Adler, F. R. (2017). Convergence in leaf size versus twig leaf area scaling: Do plants optimize leaf area partitioning? *Annals of Botany*, *119*(3), 447–456.

Spielmann, J., Ahmadi, H., Scheepers, M., Weber, M., Nitsche, S., Carnol, M., … Hanikenne, M. (2020). The two copies of the zinc and cadmium ZIP6 transporter of *Arabidopsis halleri* have distinct effects on cadmium tolerance. *Plant, Cell & Environment*, *43*, 2143–2157. https://doi.org/10.1111/pce.13806

Steffens, B., & Rasmussen, A. (2016). The physiology of adventitious roots. *Plant Physiology*, *170*(2), 603–617. https://doi.org/10.1104/pp.15.01360

Subedi, S. R., Sandhu, N., Singh, V. K., Sinha, P., Kumar, S., Singh, S. P., … Kumar, A. (2019). Genome-wide association study reveals significant genomic regions for improving yield, adaptability of rice under dry direct seeded cultivation condition. *BMC Genomics*, *20*(1), 471–471. https://doi.org/10.1186/s12864-019-5840-9

Suzuki, M., Takahashi, M., Tsukamoto, T., Watanabe, S., Matsuhashi, S., Yazaki, J., … Nishizawa, N. K. (2006). Biosynthesis and secretion of mugineic acid family phytosiderophores in zinc-deficient barley. *The Plant Journal*, *48*(1), 85–97.

Suzuki, M., Tsukamoto, T., Inoue, H., Watanabe, S., Matsuhashi, S., Takahashi, M., … Nishizawa, N. K. (2008). Deoxymugineic acid increases Zn translocation in Zn-deficient rice plants. *Plant Molecular Biology*, *66*(6), 609–617. https://doi.org/10.1007/s11103-008-9292-x

Takahashi, M., Yamaguchi, H., Nakanishi, H., Shioiri, T., Nishizawa, N. K., & Mori, S. (1999). Cloning two genes for nicotianamine aminotransferase, a critical enzyme in iron acquisition (strategy II) in graminaceous plants. *Plant Physiology*, *121*(3), 947–956. https://doi.org/10.1104/pp.121.3.947

Takahashi, R., Ishimaru, Y., Shimo, H., Ogo, Y., Senoura, T., Nishizawa, N. K., & Nakanishi, H. (2012). The OsHMA2 transporter is involved in root-to-shoot translocation of Zn and Cd in rice. *Plant, Cell & Environment*, *35*(11), 1948–1957. https://doi.org/10.1111/j.1365-3040.2012.02527.x

Takei, K., Takahashi, T., Sugiyama, T., Yamaya, T., & Sakakibara, H. (2002). Multiple routes communicating nitrogen availability from roots to shoots: A signal transduction pathway mediated by Cytokinin. *Journal of Experimental Botany*, *53*(370), 971–977. https://doi.org/10.1093/JEXBOT/53.370.971

Talke, I. N., Hanikenne, M., & Krämer, U. (2006). Zinc-dependent global transcriptional control, transcriptional deregulation, and higher gene copy number for genes in metal homeostasis of the Hyperaccumulator *Arabidopsis halleri*. *Plant Physiology*, *142*(1), 148–167.

Tennant, D. (1976). Root growth of wheat. I. Early patterns of multiplication and extension of wheat roots including effects of levels of nitrogen, phosphorus and potassium. *Australian Journal of Agricultural Research*, *27*(2), 183–183. https://doi.org/10.1071/ar9760183

The International Brachypodium Initiative. (2010). Genome sequencing and analysis of the model grass *Brachypodium distachyon*. *Nature*, *463* (7282), 763–768. https://doi.org/10.1038/nature08747

Tiong, J., McDonald, G. K., Genc, Y., Pedas, P., Hayes, J. E., Toubia, J., … Huang, C. Y. (2014). HvZIP7 mediates zinc accumulation in barley (*Hordeum vulgare*) at moderately high zinc supply. *New Phytologist*, *201*, 131–143. https://doi.org/10.1111/nph.12468

Vallee, B. L., & Falchuk, K. H. (1993). The biochemical basis of zinc physiology. *Physiological Reviews*, *73*(1), 79–118. https://doi.org/10.1152/physrev.1993.73.1.79

Vatansever, R., Filiz, E., & Eroglu, S. (2017). Genome-wide exploration of metal tolerance protein (MTP) genes in common wheat (*Triticum aestivum*): Insights into metal homeostasis and biofortification. *Biometals*, *30*, 217–235. https://doi.org/10.1007/s10534-017-9997-x

Vert, G. A., Briat, J. F., & Curie, C. (2003). Dual regulation of the Arabidopsis high-affinity root iron uptake system by local and long-distance signals. *Plant Physiology*, *132*(2), 796–804. https://doi.org/10.1104/pp.102.016089

Von Wirén, N., Marschner, H., & Romheld, V. (1996). Roots of iron-efficient maize also absorb Phytosiderophore-chelated zinc. *Plant Physiology*, *111*(4), 1119–1125. https://doi.org/10.1104/pp.111.4.1119

Walker, J. M., Tsivkovskii, R., & Lutsenko, S. (2002). Metallochaperone Atox1 transfers copper to the NH2-terminal domain of the Wilson's disease protein and regulates its catalytic activity. *Journal of Biological Chemistry*, *277*(31), 27953–27959. https://doi.org/10.1074/jbc.M203845200

Wang, H. Y., Klatte, M., Jakoby, M., Baumlein, H., Weisshaar, B., & Bauer, P. (2007). Iron deficiency-mediated stress regulation of four subgroup Ib BHLH genes in *Arabidopsis thaliana*. *Planta*, *226*(4), 897–908.

Watt, M., Schneebeli, K., Dong, P., & Wilson, I. W. (2009). The shoot and root growth of Brachypodium and its potential as a model for wheat and other cereal crops. *Functional Plant Biology*, *36*(11), 960–969. https://doi.org/10.1071/FP09214

Wintz, H., Fox, T., Wu, Y. Y., Feng, V., Chen, W., Chang, H. S., … Vulpe, C. (2003). Expression profiles of *Arabidopsis thaliana* in mineral deficiencies reveal novel transporters involved in metal homeostasis. *The Journal of Biological Chemistry*, *278*(48), 47644–47653.

Yamada, K., Nagano, A. J., Nishina, M., Hara-Nishimura, I., & Nishimura, M. (2013). Identification of two novel endoplasmic reticulum body-specific integral membrane proteins. *Plant Physiology*, *161*(1), 108–120. https://doi.org/10.1104/pp.112.207654

Yang, M., Zhang, Y., Zhang, L., Hu, J., Zhang, X., Lu, K., … Lian, X. (2014). OsNRAMP5 contributes to manganese translocation and distribution in rice shoots. *Journal of Experimental Botany*, *65*(17), 4849–4861. https://doi.org/10.1093/jxb/eru259

Yang, X., Huang, J., Jiang, Y., & Zhang, H. S. (2009). Cloning and functional identification of two members of the ZIP (Zrt, Irt-like protein) gene family in rice (*Oryza sativa* L.). *Molecular Biology Reports*, *36*(2), 281–287. https://doi.org/10.1007/s11033-007-9177-0

Yordem, B. K., Conte, S. S., Ma, J. F., Yokosho, K., Vasques, K. A., Gopalsamy, S. N., & Walker, E. L. (2011). *Brachypodium distachyon* as a new model system for understanding iron homeostasis in grasses: Phylogenetic and expression analysis of yellow stripe-like (YSL) transporters. *Annals of Botany*, *108*(5), 821–833. https://doi.org/10.1093/aob/mcr200

Zargar, S. M., Kurata, R., Inaba, S., Oikawa, A., Fukui, R., Ogata, Y., … Fukao, Y. (2015). Quantitative proteomics of Arabidopsis shoot microsomal proteins reveals a cross-talk between excess zinc and iron deficiency. *Proteomics*, *15*, 1196–1201. https://doi.org/10.1002/pmic.201400467

Zeng, H., Zhang, X., Ding, M., & Zhu, Y. (2019). Integrated analyses of miRNAome and transcriptome reveal zinc deficiency responses in rice seedlings. *BMC Plant Biology*, *19*(1), 585. https://doi.org/10.1186/s12870-019-2203-2

Zhang, Y., Chen, K., Zhao, F. J., Sun, C., Jin, C., Shi, Y., … Lian, X. (2018). OsATX1 interacts with heavy metal P1B-type ATPases and affects copper transport and distribution. *Plant Physiology*, *178*(1), 329–344. https://doi.org/10.1104/pp.18.00425

SUPPORTING INFORMATION

Additional supporting information may be found online in the Supporting Information section at the end of this article.

How to cite this article: Amini, S., Arsova, B., Gobert, S., Carnol, M., Bosman, B., Motte, P., Watt, M., & Hanikenne, M. (2021). Transcriptional regulation of *ZIP* genes is independent of local zinc status in Brachypodium shoots upon zinc deficiency and resupply. *Plant, Cell & Environment*, 1–22. https://doi.org/10.1111/pce.14151